

1 **Title:** Combined use of Oxford Nanopore and Illumina sequencing yields insights into
2 soybean structural variation biology

3

4

5 **Authors:** Marc-André Lemay^{1,2}, Jonas A. Sibbesen³, Davoud Torkamaneh^{1,2}, Jérémie Hamel^{2,4},
6 Roger C. Levesque^{2,4}, François Belzile^{1,2}

7

8 **Author affiliation**

9 1 Département de phytologie, Université Laval

10 2 Institut de biologie intégrative et des systèmes, Université Laval

11 3 UC Santa Cruz Genomics Institute, Santa Cruz, CA, USA

12 4 Département de microbiologie-infectiologie et d'immunologie, Université Laval

13

14 **Email addresses**

15 Marc-André Lemay: marc-andre.lemay.2@ulaval.ca

16 Jonas A. Sibbesen: jsibbese@ucsc.edu

17 Davoud Torkamaneh: davoud.torkamaneh.1@ulaval.ca

18 Jérémie Hamel: jeremiehamel1@hotmail.com

19 Roger C. Levesque: rclevesq@ibis.ulaval.ca

20 François Belzile: francois.belzile@fsaa.ulaval.ca (corresponding author)

21

22

23

24

25

26 **Abstract**

27 **Background**

28 Structural variant (SV) discovery based on short reads is challenging due to their complex
29 signatures and tendency to occur in repeated regions. The increasing availability of long-read
30 technologies has greatly facilitated SV discovery, however these technologies remain too costly
31 to apply routinely to population-level studies. Here, we combined short-read and long-read
32 sequencing technologies to provide a comprehensive population-scale assessment of structural
33 variation in a panel of Canadian soybean cultivars.

34 **Results**

35 We used Oxford Nanopore sequencing data (~12X mean coverage) for 17 samples to both
36 benchmark SV calls made from the Illumina data and predict SVs that were subsequently
37 genotyped in a population of 102 samples using Illumina data. Benchmarking results show that
38 variants discovered using Oxford Nanopore can be accurately genotyped from the Illumina data.

39 We first use the genotyped SVs for population structure analysis and show that results are
40 comparable to those based on single-nucleotide variants. We observe that the population
41 frequency and distribution within the genome of SVs are constrained by the location of genes.

42 Gene Ontology and PFAM domain enrichment analyses also confirm previous reports that
43 genes harboring high-frequency SVs are enriched for functions in defense response. Finally, we
44 discover polymorphic transposable elements from the SVs and report evidence of the recent
45 activity of a Stowaway MITE.

46 **Conclusions**

47 Our results demonstrate that long-read and short-read sequencing technologies can be
48 efficiently combined to enhance SV analysis in large populations, providing a reusable
49 framework for their study in a wider range of samples and non-model species.

50

51 **Keywords**

52 Structural variation, soybean genomics, Oxford Nanopore sequencing, transposable elements,
53 population studies, crop genomics, structural variant genotyping

54

55 **Background**

56 Structural variants (SVs), commonly defined as genomic variations involving at least 50
57 nucleotides, are a key source of sequence and functional variation in eukaryotes [1–4]. Indeed,
58 SVs such as deletions, insertions, duplications and inversions account for more variation in
59 sequence content than single-nucleotide variants (SNVs) in several species [e.g. 5–7]. In
60 addition to their implication in human health [8], SVs play a role in key phenotypes in crops such
61 as soybean (*Glycine max*) [9], maize (*Zea mays*) [10, 11], tomato (*Solanum lycopersicum*) [12],
62 wheat (*Triticum aestivum*) [13] and rapeseed (*Brassica napus*) [14]. Moreover, there is now
63 clear evidence for the significant role played by SVs on ecological and evolutionary processes in
64 various non-model species [15].

65

66 Despite their undeniable functional importance, genome-wide population-scale assessments of
67 SVs have lagged behind compared to SNVs due to the lack of power of short reads for SV
68 discovery [2]. Tools that discover SVs from short reads typically rely on one or several types of
69 evidence, either in the form of split reads (SV breakpoint found within an individual read),
70 discordant read pairs (unusual orientation or distance between reads of a pair), or read depth
71 (abnormally high or low coverage at a given position) [16]. Other methods rely on local or
72 genome-wide *de novo* assembly to discover SV breakpoints at base-pair resolution. These
73 methods can generally detect a larger number of SVs, but they tend to struggle with repetitive
74 SVs and on shallowly sequenced samples [17]. Unfortunately, benchmarks of tools that
75 discover SVs from short reads consistently document sub-optimal sensitivity and precision,

76 issues that can only be partly relieved by combining datasets obtained with different tools [18–
77 20].

78

79 The increased availability of long-read sequencing technologies such as Oxford Nanopore and
80 PacBio in recent years has benefited the study of SVs [21]. Indeed, their increased read length
81 allows them to both cover the span of larger variants, such as long insertions and inversions,
82 and to map more confidently in the low-complexity regions where SVs tend to occur [2]. Several
83 mapping-based methods for SV discovery from long reads have already been developed [e.g.
84 22–25] and benchmarked [26], typically performing better than methods using short reads.
85 These approaches have recently been applied to provide genome-wide assessments of SVs in
86 crops such as tomato [12], rice (*Oryza sativa*) [27] and rapeseed [28].

87

88 Despite the greater power of long reads for SV discovery, their high cost and basecalling error
89 rates make them unlikely to replace short-read technologies in the short term. In the meantime,
90 methods that allow short-read data to use the insights gained from long reads are much needed
91 in order to scale the study of SVs from the small cohorts sequenced with long-read technologies
92 up to entire populations. In particular, using short-read data to genotype SVs discovered from
93 long reads shows great promise to allow scaling up the insights gained from long reads.

94 Although methods for genotyping SVs from short reads do exist [e.g. 29–31] and have been
95 applied to SVs discovered from long-read sequencing data [e.g. 32], these approaches have yet
96 to be widely adopted in plant genomics and best practices for their application in highly
97 repetitive genomes such as that of soybean and other non-model species are still needed.

98

99 Previous studies have addressed the question of soybean structural variation using either
100 comparative genomic hybridization [33, 34], short-read sequencing [6, 35] or pan-genome
101 approaches [32, 36]. These studies have notably found evidence for an enrichment of SVs in

102 genes related to defense response [33, 34, 36] and a role of SVs in determining traits such as
103 seed coat pigmentation and iron uptake [32]. The use of a combined analysis of short and long
104 reads could nevertheless provide new insights into soybean SV biology by allowing the study of
105 sequence-resolved insertions efficiently and at a larger scale. Studies of transposable element
106 (TE) polymorphisms in soybean, for example, have been limited to the identification of TE
107 insertion boundaries [37], but long reads allow for the identification of full-length TE insertions
108 [38].

109

110 In this study, we use an approach that combines short-read and long-read sequencing to
111 improve prediction and genotyping of SVs in a soybean population. We first evaluate the overall
112 performance of predicting and genotyping SVs from short reads in soybean and identify best
113 practices for doing so. We next quantify the sensitivity and precision of genotyping Oxford
114 Nanopore-discovered SVs using Illumina sequencing data. Finally, we combine short-read and
115 long-read approaches to generate a comprehensive set of SVs from a panel of Canadian
116 soybean varieties and apply this dataset to analyze population structure, relate SV location and
117 frequency to potential impacts on gene function, and gain insights into soybean TE biology.

118

119 **Results**

120 **Benchmarking of Illumina-discovered variants**

121 Our first objective was to assess the performance of SV discovery and genotyping in soybean
122 based solely on short-read sequencing data. To do this, we merged SVs discovered using four
123 different tools (*de novo* assembly + AsmVar, Manta, smoove, and SvABA) and genotyped them
124 in 102 samples using Paragraph. The total counts of filtered calls per discovery tool, SV type,
125 and SV size class are summarized in Table 1. Genotype calls for 17 of the 102 samples were
126 compared against a truth set of SVs called from Oxford Nanopore data using Sniffles and

127 processed through a SV refinement pipeline (Additional file 1: Table S1). Comparison between
128 Paragraph genotype calls and the ground truth was performed using the sveal R package. We
129 only considered homozygous genotype calls for these benchmarks since we are analyzing
130 inbred lines.

131

132 Results show that the genotypes of deletions and insertions could be called confidently with as
133 few as two (2) supporting reads, which was used as a minimum threshold for all subsequent
134 analyses (Figure 1). At this threshold, sensitivity ranged between 50 and 65% and precision
135 ranged from 70 to 95% for deletions, while sensitivity ranged between 30 and 40% and
136 precision ranged from 65 to 85% for insertions (Figure 1). Precision was typically higher for
137 intermediate-sized deletions (100-10,000 bp) than for either extremes, while sensitivity was
138 highest for smaller ones (50-1,000 bp). Precision was higher for larger insertions than for small
139 ones, at the expense of lower sensitivity; virtually no insertions larger than 1 kb could be called
140 from the Illumina data (Table 1). Sensitivity increased markedly when repetitive regions were
141 ignored, with sensitivity increasing by up to 10-20% depending on the SV type and size class,
142 while precision remained roughly similar (Additional file 1: Figure S1). Results for inversions
143 showed moderate precision (in the range of 40-70%) and low sensitivity (range of 10-20%),
144 while results for duplications showed both low precision (range of 10-20%) and sensitivity (15-
145 20%) (Additional file 1: Figure S2). Poor performance was expected for inversions and
146 duplications given the high complexity of those types of SVs. Excluding repeat regions did little
147 to improve the results for duplications, but it did improve sensitivity by roughly 10% for
148 inversions (Additional file 1: Figure S3). We observed a correlation between the Oxford
149 Nanopore sequencing depth and the genotyping precision of deletions, insertions and
150 duplications for a given sample, with this effect being most important for duplications (Additional
151 file 1: Figure S4). This suggests that samples that were less deeply sequenced with long reads
152 may have failed to reveal some SVs, thus resulting in a seemingly lower precision.

153

154 Next, we assessed whether filtering SVs based on their frequency in the population resulted in a
155 higher-quality SV set by removing putative false variants. Precision-recall curves computed for a
156 range of homozygous ALT count (see Methods for more details) thresholds indicated that a filter
157 based on a minimum of four alternate alleles observed across the population yielded a good
158 compromise between sensitivity and precision for insertions and deletions (Additional file 1:
159 Figure S5). This threshold was used to filter the set of SVs for all downstreams analyses.
160 Filtering on the homozygous ALT count did not succeed in significantly increasing the
161 genotyping performance of duplications and inversions (Additional file 1: Figure S6), so we
162 decided to drop these SVs from downstream analyses. We also investigated whether a filter
163 based on the number of distinct tools reporting a SV could be used to improve sensitivity and
164 precision (Additional file 1: Figure S7). However, the drop in sensitivity when requiring more
165 than one tool was generally too large to compensate for the increase in precision. Researchers
166 valuing precision over sensitivity could however use this filter, as the gain in precision was
167 considerable in some cases, like for large deletions.

168

169 As a consequence of their different approaches to SV discovery, and consistently with the drop
170 in sensitivity observed when requiring multiple calling tools to consider a variant (Additional file
171 1: Figure S7), the various tools used showed different profiles in terms of the number of variants
172 of different sizes and types discovered (Additional file 1: Figure S8). The performance of the
173 different tools used for calling SVs is shown for a single representative sample in figures S9 and
174 S10 (Additional file 1). Manta was the most important contributor of unique true positive SV calls
175 for both deletions and insertions, followed by AsmVar. There is an obvious decrease in the false
176 positive rate when combining evidence from several calling tools. However, individual tools still
177 made significant contributions that justified their inclusion, with the exception of SvABA
178 insertions which contributed few true positive SVs compared to the number of false positives

179 (Additional file 1: Figure S10). SvABA insertions were still used for downstream analyses, but
180 could be excluded for applications where the need for precision outweighs the need for
181 sensitivity.

182

183 **Re-genotyping Oxford Nanopore-discovered variants**

184 In addition to using the SVs discovered from the Oxford Nanopore data as a truth set for
185 benchmarking SV discovery, we also assessed whether these could be accurately genotyped
186 using Illumina data. For that purpose, we merged the calls made from the Oxford Nanopore
187 data of all 17 samples using SVmerge. These were used as input to Paragraph and re-
188 genotyped using Illumina data from the same 17 samples. The genotypes were compared to the
189 SV calls made by Sniffles directly from the Oxford Nanopore data results using the sveval
190 package as was done for the Illumina SVs.

191

192 As was the case for Illumina SVs, two (2) Illumina reads were sufficient to confidently call SVs in
193 most samples (Figure 2). At this threshold, sensitivity ranged from 55 to 65% and precision
194 ranged between 80 and 95% for deletions, while sensitivity ranged from 50 to 60% and
195 precision ranged between 60 and 80% for smaller insertions (Figure 2). For deletions, sensitivity
196 and precision were fairly consistent across size classes. For insertions, however, precision
197 varied immensely from 20% to ~80% for 1-10 kb insertions and from essentially 0 to 60% for
198 insertions larger than 10 kb. Further analysis showed that there was a correlation between the
199 precision of insertion genotyping in these size classes and the N50 of Oxford Nanopore reads of
200 a given sample (Additional file 1: Figure S11). Therefore, it is likely that the poor precision
201 observed for some samples is the result of limitations of the truth dataset rather than true
202 genotyping errors. Indeed, larger insertions could not be validated in low-N50 samples because
203 the small length of the reads prevented their discovery in those samples. Yet, those large
204 insertions could still be genotyped using the Illumina data provided that they were discovered in

205 other samples with higher N50. As was the case for variants discovered from the Illumina data,
206 sensitivity was higher when we excluded repeat regions, with sensitivity reaching 80% in some
207 cases (Additional file 1: Figure S12).

208

209 Duplications discovered by Sniffles showed low sensitivity and precision with both being in the
210 20-40% range (Additional file 1: Figure S13a). Inversions, however, could be accurately
211 genotyped from the Illumina data, with a precision typically greater than 70%, but their
212 sensitivity was low at about 10-20% (Additional file 1: Figure S13b). Concentrating on non-
213 repeat regions moderately improved the results for duplications (Additional file 1: Figure 14a)
214 but did so to a larger extent for inversions, with sensitivity reaching over 20% and precision
215 being generally over 80% (Additional file 1: Figure S14b).

216

217 **Population-scale genotyping of the joint Oxford Nanopore-Illumina SV dataset**

218 In order to produce a population-scale SV dataset that could be used for downstream analyses,
219 we merged the SVs discovered from the Illumina and Oxford Nanopore data using SVmerge
220 and genotyped them with Paragraph using the Illumina data of the 102 samples. Benchmarking
221 results for deletions and insertions expectedly showed a precision that was in-between that of
222 the previous two benchmarks (Illumina SVs and Oxford Nanopore SVs), both when considering
223 all regions (Additional file 1: Figure S15) and non-repeat regions only (Additional file 1: Figure
224 S16).

225

226 The dataset was further filtered using knowledge gained from the previous benchmarks.
227 Namely, we filtered out genotype calls with fewer than two (2) supporting reads and removed
228 SVs with fewer than four (4) alternate alleles observed among homozygous genotype calls
229 (homozygous ALT count). Inversions and duplications were also removed for downstream
230 analyses due to their poor performance in the benchmarks.

231

232 The distribution of deletion and insertion calls within the reference genome is illustrated in
233 Figure 3c. There is a visible tendency for SVs to be more frequent in gene-rich euchromatic
234 regions (Figure 3a) where predicted SNVs are also more densely distributed (Figure 3b),
235 although this may be due only to a higher discovery power in euchromatic regions. The
236 presence of SV hotspots on chromosomes 3, 6, 7, 16 and 18 (Figure 3c) is consistent with
237 results previously obtained using comparative genomic hybridization by McHale et al. [34] and
238 by a pan-genome approach [36].

239

240 **Population structure**

241 To assess the quality of our population-scale SV dataset, we verified whether population
242 structure inferred from SVs yielded similar results to that inferred from SNVs, which are more
243 commonly used for population structure inference. For this purpose, we assigned all individuals
244 to one of five (5) populations using fastStructure with SNV data first, and then performed
245 principal component analysis (PCA) on both SNV and SV data using PLINK.

246

247 The PCAs did not cluster the samples belonging to different populations into starkly distinct
248 groups because the panel under study does not display a strong structure to begin with. Still,
249 both the SV (Additional file 1: Figure S17a) and the SNV PCA (Additional file 1: Figure S17b)
250 roughly grouped individuals according to their assigned population. Moreover, the PCA made
251 from the SV genotype calls was at least as good at clustering together the samples belonging to
252 the same population as the PCA made using SNVs was. Overall, these results constitute a
253 proof of concept that the population-scale SV dataset is the reflection of a biological reality and
254 not an artifact.

255

256 **Potential impact on genes**

257 SVs can have a large impact on gene integrity or expression. Therefore, we annotated the SVs
258 in our dataset according to the genic features they overlapped. SVs occurred disproportionately
259 less within coding sequences than would be expected based on the proportion of the genome
260 covered by these features, both when considering the whole genome and when restricting the
261 analysis to non-repeat regions (Additional file 1: Table S2). A slight underrepresentation of SVs
262 was also observed within non-coding genic sequences, although this pattern was much clearer
263 when concentrating on non-repeat regions. Both analyses also revealed a clear pattern of
264 overrepresentation of SVs within regions 5 kb upstream of genes. The proportion of SVs
265 overlapping intergenic regions appeared to be less than expected when the analysis was
266 performed on the whole genome, but this is most likely due to the fact that intergenic regions
267 tend to be more repetitive and thus more difficult to probe. Indeed, when restricting the analysis
268 to non-repeat regions, the proportion of SVs falling within intergenic regions was higher than
269 their proportion within the reference genome, suggesting enrichment of SVs. We also compared
270 the observed proportions of SVs overlapping various genic features to what would be expected
271 by random chance using a randomization test that shuffled the positions of SVs within 100-kb
272 bins and computed the resulting overlaps. The 100-kb bins were used to locally restrict the SVs
273 position to take into account the repeat heterogeneity of the genome. This test confirmed the
274 underrepresentation of SVs within coding sequences and their overrepresentation within
275 intergenic sequences and regions 5 kb upstream of genes (Figure 4a). The pattern for non-
276 coding genic sequences, however, diverged from other lines of evidence by suggesting slight
277 overrepresentation of deletions. Insertions, on the other hand, appeared to be underrepresented
278 within non-coding genic sequences, similar to the results shown in Table S2 (Additional file 1).
279
280 The distributions of insertion and deletion frequencies depending on the features overlapped are
281 shown in Figure 4b. Statistical testing of the pairwise differences in mean SV frequencies
282 depending on the genic features overlapped clearly showed that deletions overlapping coding

283 sequences were less frequent (the frequency being lower by roughly 0.05) than those occurring
284 elsewhere in the genome (Additional file 1: Table S3). For insertions, the only significant
285 differences indicated a higher frequency (by roughly 0.02) in intergenic regions than in non-
286 coding genic sequences or sequences 5 kb upstream of genes. A difference of similar
287 magnitude was also observed between mean insertion frequency within intergenic regions and
288 coding sequences, but the difference was marginally non-significant.

289

290 Finally, we conducted an enrichment analysis to check for over- and underrepresentation of
291 gene ontology (GO) Biological Process terms and PFAM protein domains in genes whose
292 coding sequence is impacted by SVs that are frequent (≥ 0.5) in the population. Genes
293 impacted by high-frequency SVs were highly enriched for functions involved in defense
294 response, and somewhat less so for functions involved in the regulation of various pathways
295 (Additional file 1: Table S4; Additional file 2). Underrepresented GO Biological Process terms
296 were almost all related to various metabolic or biosynthetic processes (Additional file 1: Table
297 S5; Additional file 3). As was observed for GO Biological Process terms, the PFAM domain
298 enrichment analysis showed that genes impacted by high-frequency SVs are overwhelmingly
299 enriched in domains involved in defense response, such as NB-ARC, TIR and Leucine rich
300 repeat domains (Additional file 1: Table S6; Additional file 4). No PFAM domains were observed
301 to be underrepresented (Additional file 5).

302

303 **Transposable elements**

304 Many SVs, especially larger ones, result from the mobilization of TEs [12, 39]. With this in mind,
305 we checked whether we could gain insights into soybean TE biology from our SV dataset. To do
306 so, we first queried the sequences of all insertions and deletions larger than 100 bp in our
307 dataset against a database of soybean TEs. Insertions and deletions that matched a TE with
308 high confidence were annotated with the corresponding TE type.

309

310 A total of 2,586 deletions and 2,391 insertions were annotated as TEs by this approach (Table
311 2; Figure 3d,e; Additional file 6). These represent 8.4% and 9.1% of all deletions and insertions,
312 respectively, and 14.9% and 17.4% of those larger than 100 nucleotides. The proportion of
313 polymorphic TEs of different classes found within our dataset is consistent with their prevalence
314 in the reference genome, except for DNA TEs which represent a much smaller proportion of the
315 polymorphic elements compared to their prevalence in the genome. The number of polymorphic
316 elements per LTR-retrotransposon family (Figure 5a) and per DNA TE type (Figure 5b) were
317 largely consistent with results previously reported for non-reference soybean TEs [37] except for
318 DNA TEs of the CACTA superfamily for which we found almost no polymorphic instances.

319

320 We identified terminal inverted repeat (TIR) and target site duplication (TSD) sequences from
321 local assemblies of the TE sequences for 40 different polymorphic SVs collectively representing
322 17 entries in the SoyTEdb database. The polymorphic TEs for which we could identify TIR and
323 TSD sequences were essentially miniature inverted-repeat transposable elements (MITEs)
324 ranging in size from 198 to 681 bp (longer sequences were too challenging to assemble
325 properly). From these data, we computed the proportion of matching nucleotides between the
326 two inverted repeats and averaged the values over the all samples bearing the TE insertion for
327 a given SV (Figure 5c). A high proportion of matching nucleotides can indicate the potential for
328 active transposition because intact transposons should have identical or nearly identical TIRs.
329 While the proportion of matching nucleotides was under 0.8 in most cases, three polymorphic
330 TEs matching the Tc1-Mariner superfamily and annotated as Stowaway MITEs presented a
331 proportion of matching nucleotides > 0.9 (Additional file 7).

332

333 We generated multiple alignments of the local assemblies at all sites where at least one sample
334 had recognizable TIR and TSD sequences. A visual analysis of these multiple alignments

335 revealed that for all but one SV, the sequences that did not bear the insertion presented a single
336 occurrence of the TSD sequence. This observation is consistent with a scenario where the TE
337 never inserted into the sequence, instead of having excised from it. The one exception to this
338 observation is that of a 480-bp insertion of a Stowaway MITE at position 2,257,090 of
339 chromosome Gm04. In this case, a visual analysis of the multiple alignment revealed that three
340 different alleles are segregating in the population at the insertion site: (1) the reference allele (no
341 insertion at the target position), (2) a 480-bp insertion that corresponds to the TE insertion, and
342 (3) a 6-bp insertion of nucleotides TACGAG (Additional file 1: Figure S18; Additional file 8).
343 Interestingly, this insertion is by far the one for which the percent similarity between the two TIR
344 sequences was highest among the ones studied, at 96.3%. We hypothesized that the 6-bp
345 insertion resulted from the excision of the TE, with the TA nucleotides being remnants of the
346 classical Tc1-Mariner TSD and the other nucleotides having been added during DNA repair
347 following excision. If this is the case, then the haplotypes surrounding the insertion site should
348 be very similar between the individuals with the TE insertion and those with the 6-bp insertion.
349 Using a combination of SV calls made by Paragraph and indel calls made by Platypus, we
350 assigned 71 individuals as homozygous for the reference allele, 9 individuals as homozygous
351 for the TE insertion allele and 14 individuals as homozygous for the 6-bp insertion allele. We
352 computed the alternate allele frequencies within each of these three groups for 156 SNVs
353 located in a 39-kb linkage disequilibrium block surrounding the insertion site (Figure 5d). The
354 results clearly show high genetic similarity between individuals bearing the TE insertion and
355 those bearing the 6-bp insertion, consistent with the latter being derived from excision of the TE
356 insertion. In fact, only three (3) SNVs showed contrasting allele frequencies (difference in allele
357 frequencies > 0.5) between these two groups (Figure 5d), whereas 129 alleles were contrasted
358 between the reference allele haplotype and the TE insertion allele haplotype. This suggests that
359 the excision of the TE is a relatively recent event and that this TE may still be active in soybean.
360

361 Interestingly, one of the polymorphic *Copia* insertions found in our dataset matches an insertion
362 in the Glyma.20G090000 gene (also known as the PhyA2 gene corresponding to the E4
363 maturity locus) known to impact time to maturity in soybean [40]. In our dataset, this TE
364 insertion had a frequency of 0.207, with 20 samples genotyped as homozygous for the
365 alternative allele and a single one genotyped as heterozygous.

366

367 **Discussion**

368 The rapid development of long-read sequencing platforms such as PacBio and Oxford
369 Nanopore in recent years has greatly enhanced the potential for studying structural variation.
370 Although studies using long reads to survey structural variation in crops have started to emerge
371 [e.g. 12, 27, 28], they did not explicitly address the question of using short reads to scale up SV
372 analysis from the small cohorts sequenced using long reads to larger populations, as has been
373 done in humans [e.g. 41, 42]. This question is of interest because long-read sequencing
374 remains too expensive at the moment to apply at large scale and because large amounts of
375 already-existing short-read sequencing data could be leveraged in that way. Scaling up the
376 study of SVs is a necessary prerequisite to getting a clear understanding of genome evolution
377 and function, and applying this knowledge to real-world problems [1, 15]. In this study, we
378 demonstrate that a relatively small cohort of 17 samples sequenced to ~12X coverage with
379 Oxford Nanopore can be combined with Illumina data to drive the study of SVs in a population
380 of 102 Canadian soybean lines and gain insights into SV biology.

381

382 The SVs discovered from short-read sequencing data are typically limited to variants located in
383 non-repeated regions and relatively small insertions (< 200 bp). These results have been shown
384 repeatedly by benchmarking studies [18, 20] and reflect an inherent limitation of short reads to
385 span large repeats and effectively assemble into long insertions. Here, we still used Illumina

386 reads for SV discovery to survey the whole population and thus detect less frequent variants
387 that may not have been found within the 17 samples sequenced with Oxford Nanopore data.
388 However, despite following recommended practices for SV analysis such as combining different
389 SV calling tools and integrating the results with a dedicated SV genotyper, estimated sensitivity
390 for insertions remained low at ~40% for those in the range 50-100 bp and ~30% for those in the
391 range 100-1,000 bp. The improved sensitivity obtained when focusing on non-repeated regions
392 (up to ~60% for insertions in the range 50-100 bp) shows that a large part of the problem indeed
393 comes from repeated regions. However, entirely removing these regions from analyses is an
394 unsatisfactory solution as polymorphisms in these regions may still be relevant to a particular
395 study question.

396

397 To compensate for limitations in SV discovery from short reads, we assessed whether Illumina
398 reads could be used to genotype SVs discovered from Oxford Nanopore data on a smaller
399 cohort of 17 samples. The greatest added value of this approach arguably comes from the
400 possibility to accurately genotype large (> 1 kb) insertions with > 70% sensitivity. This is an
401 encouraging result because it shows that such insertions can be successfully genotyped using
402 Illumina data even though they could not be discovered from this same data. This is because
403 long reads provide the full contiguous sequence of insertions, which the Illumina reads can then
404 map to. Combined with a novel pipeline for refining the breakpoints and sequence content of
405 SVs discovered from Oxford Nanopore sequencing data prior to genotyping, this approach
406 should enable the study of SVs in large populations for which short-read data is already
407 available. The main limitation to using this approach actually comes from the long-read data
408 itself. In this study, some of the samples appeared to have low genotyping precision for larger
409 insertions, but this was most likely due to these insertions not being discovered in samples with
410 lower read N50 and thus appearing as false positive genotype calls. Similarly, the sequencing
411 depth of the Oxford Nanopore data used here was not sufficient to provide a solid reference

412 dataset for benchmarking duplications. Indeed, one limitation of our study is that Oxford
413 Nanopore reads alone do not provide a perfect ground truth for benchmarking, especially for
414 SVs under 100 bp [2], but this was the best truth set we had access to in the absence of a gold
415 standard SV dataset for soybean.

416

417 Follow-up analysis on our population-scale SV dataset confirmed that this dataset reproduced
418 previously described population structure patterns, an validation approach commonly used in
419 other population-scale SV studies [e.g. 43, 44]. We indeed found that a PCA using SVs
420 summarized the population structure just as well as a PCA using SNVs, which indicates that the
421 SV genotype calls on the 102-sample population are accurate. Perhaps more importantly, the
422 SV dataset produced here met our expectations regarding the genome-wide distribution of SVs
423 and their location relative to predicted gene models. The location of SV hotspots found here is
424 consistent with previously reported results [34, 36]. Moreover, GO term and PFAM domain
425 enrichment analyses confirmed previous observations that SV-enriched genes were involved in
426 plant defense response [33, 34, 36]. Several lines of evidence in our results also suggest a
427 strong functional constraint on the location of SVs in the soybean genome. Notably, SVs were
428 strongly depleted within coding sequences compared to what would be randomly expected, and
429 insertions were depleted within non-coding genic sequences. There was also a clear tendency
430 for enrichment of SVs in regions upstream of genes, but whether this is simply due to lower
431 functional constraints or a role of SVs in regulating gene expression remains to be investigated.
432 Functional constraints on the frequency of SVs could also be observed from our data, as
433 deletions impacting coding sequences were less frequent than those occurring elsewhere in the
434 genome and insertions were enriched within intergenic regions, which are arguably less
435 functionally important. Based on these results, we suggest that many of the deletions located
436 within coding sequences may have a deleterious impact and could therefore become targets for
437 breeding.

438

439 The large insertions and higher power of SV discovery within repetitive regions that was
440 afforded by the Oxford Nanopore sequencing data gave us an opportunity to study soybean TE
441 biology more deeply than previous reports. The numbers of TEs associated with various
442 superfamilies was largely consistent with results previously reported by Tian et al. [37], except
443 for DNA TEs of the CACTA superfamily which were a lot less common in our data. We observed
444 the same pattern of general concordance with previously reported results except for CACTA
445 elements when comparing our data to that of Istanto [45]. The reason why we found almost no
446 polymorphic CACTA elements compared to these studies is unclear, but we hypothesize that it
447 may be due to our more stringent requirements for TE annotation. Indeed, we required the
448 length of the queried SVs to be close to that of their matching counterpart in the database. Many
449 of the SVs in our dataset indeed matched CACTA elements following the BLASTN query, but
450 almost all of them failed to pass the filter. Our annotation results are probably conservative for
451 other types of TEs as well because the database we used is likely incomplete, as it is based on
452 the analysis of a single reference genome.

453

454 Our data also allowed us to generate original findings related to DNA TEs in soybean, which
455 have received relatively little attention from past studies. We report results that suggest that
456 most DNA TE insertion polymorphisms in soybean result from past insertion of TEs rather than
457 from excision of existing TEs. The relatively low proportion of polymorphic DNA TEs compared
458 to their prevalence in the genome also suggests that these elements are overall fairly inactive in
459 soybean. However, we did document one case in which recent excision of a Stowaway MITE
460 from its insertion site appears to have occurred, such that three alleles (the reference allele
461 without the insertion, the TE insertion, and the allele resulting from the excision of the TE) are
462 present within the population. This element represents a prime candidate to study the potential
463 activity of DNA TE transposons in soybean.

464

465 **Conclusions**

466 In conclusion, our study shows that Oxford Nanopore and Illumina sequencing data can be
467 efficiently combined to study structural variation in soybean. In particular, large insertions that
468 cannot be discovered from short-read data alone could be genotyped using short-read data and
469 thus allow the insights gained from long-read sequencing to scale up to a larger population. This
470 approach, combined with a novel pipeline for refining the SVs discovered using Oxford
471 Nanopore data, should extend easily to other species and allow the wealth of already-existing
472 Illumina data to be leveraged for SV analysis. In addition to confirming previous results
473 regarding the chromosomal distribution of SVs in soybean and their association with genes
474 involved in defense response, we also report novel insights into functional constraints to the
475 occurrence of SVs and into soybean TE biology. Moreover, the SV catalog described here is
476 freely available and can be used as a resource for SV genotyping by the soybean research
477 community. These results as well as the framework developed to optimize the study of structural
478 variation at population scale should help to better integrate these variants in genomic studies of
479 crops and other non-model species.

480

481 **Methods**

482 **Illumina sequencing and read processing**

483 Sample selection and acquisition of Illumina sequencing data has been described in previous
484 work [6]. Briefly, 102 Canadian soybean cultivars and breeding lines were selected to
485 encompass the full range of genetic variation found among Canadian short-season germplasm
486 and sequenced on the Illumina HiSeq 2500 platform. Paired-end reads ranging in size from 100
487 to 125 nucleotides were obtained depending on the sample. This sequencing data is available
488 on the NCBI Sequence Read Archive (SRA) through BioProject accession number

489 PRJNA356132 [46].

490

491 All reads were adapter- and quality-trimmed using bbduk from the BBtools suite v. 38.25 [47].

492 We aligned reads using bwa mem v. 0.7.17-r1188 [48] with default parameters. Paired-end

493 alignment mode was used except for reads that were left unpaired following adapter and quality

494 trimming, which were aligned in single-end mode. We used a reference genome consisting of

495 assembly version 4 of the Williams82 reference cultivar [49] concatenated with reference

496 mitochondrion and chloroplast sequences retrieved from SoyBase [50]. Reads aligned using

497 paired-end and single-end mode were then merged, sorted and indexed using samtools v. 1.8

498 [51] and read groups were added using bamaddrg [52]. The sorted and indexed BAM files were

499 used as input for all downstream analyses requiring mapped reads.

500

501 **Structural variation discovery from short reads**

502 We called SVs on all 102 samples using four different tools: AsmVar [53], Manta [54], SvABA

503 [55], and LUMPY-based [56] smoove [57]. We selected this combination of tools based on the

504 complementarity of their SV detection approaches, widespread use within the community, and

505 performance reported in published benchmarks [20].

506

507 AsmVar calls SVs by comparing *de novo* genome assemblies to a reference genome. Prior to

508 assembly, we merged reads that were still paired after trimming using FLASH v. 1.2.11 [58].

509 The rationale behind this was that the short size of the inserts in our sequencing data allowed

510 several of the read pairs to be merged into longer sequences. Reads were grouped into three

511 libraries (single-end reads from bbduk, single-end reads merged by FLASH, and paired-end

512 reads left unmerged by FLASH) and assembled with SOAPdenovo2 v. 2.04 [59] using the

513 sparse_pgraph and contig commands, and a k-mer size of 49. Contigs were not further

514 assembled into scaffolds because we aimed to only call SVs whose sequence was entirely

515 resolved. The resulting contigs were aligned to the reference genome using LAST v. 1047 [60]
516 by first calling the lastal command with options -D1000 -Q0 -e20 -j4 and then the last-split
517 command with options -m 0.01 -s30. Variants were called on the LAST alignments using
518 ASV_VariantDetector from the AsmVar tool suite (version of 2015-04-16) with default
519 parameters. The pipeline was run on each sample independently and results were subsequently
520 concatenated to obtain a single AsmVar VCF file. Variants with a FILTER tag other than “.” were
521 filtered out from the resulting call set.

522

523 We ran manta v. 1.6.0 with default parameters in 10 batches of 10 or 11 randomly grouped
524 samples because it did not scale well to the whole population. We used the candidate SVs (and
525 not the genotype calls themselves) identified by each run for further processing and filtered
526 them by removing unresolved breakends (SVTYPE=BND). The filtered variants were then
527 converted from symbolic alleles (i.e. DEL, DUP, INS) to sequence-explicit ALT alleles using
528 bayesTyperTools convertAllele v. 1.5 [31] and combined into a single VCF file using bcftools
529 merge (version 1.10.2-105) [51].

530

531 We ran SvABA v. 1.1.3 separately on all samples using the command svaba run with options --
532 germline -I -L 6. SvABA produces two different variant sets: one for indels, which are already
533 coded as sequence-explicit, and another for SVs which are coded as paired breakends. We
534 therefore classified SVs into defined types (DEL, DUP, INV) based on breakpoint orientation
535 and converted them to sequence-specific ALT alleles using an in-house R script. The resulting
536 sequence-explicit variants were merged using bcftools merge.

537

538 We ran smoove v. 0.2.4 on all samples using a series of commands. First, smoove call was run
539 separately on each sample using default parameters. The variants identified were then merged
540 into a single VCF file using smoove merge, smoove genotype with options -x -d, and smoove

541 paste. Symbolic alleles (, <DUP> and <INV> alleles) were converted to explicit sequence
542 representation using bayesTyperTools convertAllele.

543

544 A series of common filters were applied to the SV output of all four tools before using them for
545 downstream analyses. Specifically, we removed variants spanning less than 50 bp or more than
546 500 kb, those located on unanchored scaffolds or organellar genomes, or any variant that was
547 not classified as either a deletion, insertion, duplication or inversion. We also converted
548 multiallelic variants into biallelic records and standardized the representation of all alleles using
549 bcftools norm.

550

551 **Oxford Nanopore sequencing**

552 We selected 17 samples for Oxford Nanopore sequencing among those sequenced by Illumina.
553 Sixteen (16) of them were randomly selected among a subset of 56 lines belonging to a core set
554 of Canadian soybean germplasm, while the remaining sample (CAD1052/OAC Embro) had
555 been selected and sequenced before the others based on its higher Illumina sequencing depth.
556 Although sample selection did not explicitly maximize the number of potential SVs assessed, we
557 did verify that the resulting set covered the range of variation found in Canadian soybean
558 germplasm based on an existing phylogenetic tree [6].

559

560 Our sample preparation and sequencing protocols evolved throughout the project as we gained
561 experience with Oxford Nanopore sequencing. Therefore, we outline our latest methods here,
562 but more details regarding the procedures used for each sample can be found in Table S7
563 (Additional file 1). Accessions selected for sequencing were germinated in Jiffy peat pellets (Jiffy
564 Group, Zwijndrecht, Netherlands) on the benchtop. Young trifoliate leaves were collected
565 between two and three weeks after germination, flash frozen in liquid nitrogen upon harvest and
566 stored at -80 °C until DNA extraction. Single trifoliate leaves weighing between 20 and 60 mg

567 were used for each extraction. Liquid nitrogen-frozen leaves were pulverized on a Qiagen
568 TissueLyser instrument (Qiagen, Hilden, Germany) with metal beads for four cycles of 30 s
569 each at 30 Hz. The resulting powder was immediately transferred to a CTAB buffer (2% CTAB,
570 0.1 M Tris-HCl pH 8, 0.02 M EDTA pH 8, 1.4 M NaCl, 1% (m/v) PVP) and incubated at 60°C in
571 a water bath for 45 min. The lysate recovered after centrifugation at 3500 rcf for 10 minutes was
572 then subjected to an RNase A treatment for another 45 min at 60°C, followed by the addition of
573 an equal volume of 24:1 chloroform:isoamyl alcohol to the sample and stirring to an emulsion.
574 Following centrifugation at 3500 rcf for 15 minutes, the supernatant was recovered and mixed
575 with a 0.7 volume of cold isopropanol. This mix was stored at -80°C for 20 minutes and
576 centrifuged at 3500 rcf for 30 min, after which the liquid was removed. Tubes were rinsed twice
577 with cold 70% ethanol, with a centrifugation step after each addition of ethanol. After the last
578 rinsing, tubes were left to dry for 3 minutes after which pellets were resuspended in 100 µl
579 elution buffer (Tris-HCl 0.01 M and EDTA 0.001 M, pH 8) at 37°C for an hour, and then stored at
580 4°C until use.

581

582 Samples were size-selected using the Short Read Eliminator kit of Circulomics (Circulomics,
583 Baltimore, MD, USA) following the manufacturer's instructions. The size-selected DNA
584 resuspended in the SRE kit's EB buffer was then purified using SparQ magnetic beads and
585 resuspended in ddH₂O. Typically, between 500 ng and 1 µg of this DNA was used for Oxford
586 Nanopore library preparation using the SQK-LSK109 genomic DNA ligation kit (Oxford
587 Nanopore Technologies, Oxford, UK). The library was prepared according to the manufacturer's
588 instructions except for the following details: 1) DNA fragmentation was not performed prior to
589 library preparation, 2) 80% ethanol was used instead of 70% ethanol, 3) the bead elution time
590 following DNA repair and end-prep was increased from 2 min to 10 min, 4) the bead elution time
591 following adapter ligation and clean-up was increased from 10 to 15 minutes and carried out in a
592 water bath set to 37°C. Typically, between 150 ng and 400 ng of the prepared library quantified

593 using a Qubit fluorometer (Thermo Fisher Scientific, Waltham, MA, USA) were used as input to
594 a FLO-MIN106D flowcell (R9 chemistry) and run on a MinION for 48 to 72 hours using default
595 voltage settings. While most accessions were sequenced on a single flow cell, three accessions
596 for which the initial yield was low (< 9 Gb) were sequenced a second time (using DNA from a
597 different plant) to provide sufficient data for downstream analyses. More details regarding the
598 Oxford Nanopore sequencing of the samples can be found in Table S8 (Additional file 1).

599

600 **Structural variation discovery from Oxford Nanopore data**

601 Raw FAST5 sequencing files were basecalled on a GPU using Oxford Nanopore Technologies'
602 guppy basecaller v. 4.0.11 with parameters --flowcell FLO-MIN106 --kit SQK-LSK109.
603 Basecalled FASTQ files obtained from a single flow cell were concatenated into a single file
604 which was used for downstream analyses. Adapters were trimmed using Porechop v. 0.2.4 [61]
605 with the option --discard_middle. Adapter-trimmed reads were aligned using NGMLR v. 0.2.7
606 [24] with the option -x ont. The resulting alignments were sorted and indexed using samtools.

607

608 At this stage, we merged the BAM files of samples that were sequenced on two different
609 flowcells and called SVs using Sniffles v. 1.0.11 [24]. We ran Sniffles with parameters --
610 min_support 3 (minimum number of reads supporting a variant = 3, default = 10), --
611 min_seq_size 1000 (minimum read segment length for consideration = 1000, default = 2000)
612 and --min_homo_af 0.7 (minimum alternate allele frequency to be considered homozygous =
613 0.7, default 0.8). We chose relaxed parameters compared to the defaults because our samples
614 are inbred cultivars and heterozygosity should therefore be nearly non-existent.

615

616 We applied a series of filters to the SVs in order to remove any spurious calls that could affect
617 downstream analyses. Any variants called on organellar genomes or unanchored scaffolds were
618 filtered out, along with any variants smaller than 50 nucleotides or larger than 500 kb. We only

619 retained deletions, insertions, inversions and duplications for further analyses, discarding
620 unresolved breakpoints (SVTYPE=BND) as well as other complex types such as DEL/INV,
621 DUP/INS, INVDUP and INV/INVDUP. We removed variants called as heterozygous since
622 heterozygous genotype calls are very likely to be spurious in these inbred lines. In order to
623 avoid calling artificial variants in ambiguous regions of the genome (stretches of “N” due to
624 imperfectly assembled regions of the reference genome), we also removed deletions that
625 overlapped any “N” in the reference as well as any insertion located less than 20 nucleotides
626 away from any “N” in the reference.

627

628 The location of SVs as well as the insertion sequences reported by Sniffles are necessarily
629 imperfect as they are based on error-prone Oxford Nanopore reads (on average 8-10% error
630 rate based on the percent identity of our alignments). We therefore assembled a pipeline to
631 refine the breakpoint location and the sequence content of the deletions and insertions found by
632 Sniffles. Duplications and inversions were not considered for SV refinement because the
633 inherent complexity of these variants made it difficult to accurately assemble them from our
634 data. We briefly describe the pipeline here, but more details can be found in Additional file 1
635 (Supplemental Methods, Table S9 and Figures S19 to S21). Our breakpoint refinement pipeline
636 starts by locally assembling all reads that were mapped by NGMLR to positions \pm 200 bp from
637 the location of the SV using wtdbg2 v. 2.5 [62]. The same reads are then aligned to the
638 assembled sequence using minimap2 v. 2.17-r974 [63] to polish the assembly sequence using
639 the consensus module of wtdbg2. The resulting polished assembly is subsequently aligned to
640 the local region of the reference genome using AGE (commit 6fa60999,
641 github.com/abzovlab/AGE) [64]. The coordinates of the SV and insertion sequence content are
642 then optionally updated from the information provided by the AGE alignment. When the
643 alignment did not suggest suitable replacement coordinates or insertion content for a given SV,
644 we simply used its representation as initially defined by Sniffles for downstream analyses

645 instead. Following breakpoint refinement, the representation of the alleles was standardized
646 using bcftools norm.

647

648 **Structural variant genotyping and benchmarking**

649 We genotyped SVs on all 102 Illumina samples using Paragraph v. 2.4a [29] in three different
650 batches. The first batch used only variants discovered from the Illumina data as input and was
651 used to assess the performance of SV discovery from Illumina data alone. The second batch
652 used only variants discovered from Oxford Nanopore data and was similarly used to assess the
653 performance of genotyping those variants with Illumina data. The third and last genotyping
654 batch used a merged dataset comprising both variants discovered using Illumina and Oxford
655 Nanopore data, and was used for the population-scale analyses on population structure,
656 location of variants relative to gene models, and polymorphic TEs. Despite the superior
657 performance of long-read data for SV discovery, we decided to also include variants discovered
658 from the Illumina data in the final SV set as they encompassed all samples.

659

660 For genotyping SVs discovered from Illumina data, the VCF files of all discovery tools (AsmVar,
661 Manta, SvABA, smoove) were merged together using SVmerge (commit 6a18fa3d2,
662 github.com/nhansen/SVanalyzer) [65] with parameters -maxdist 15 -reldist 0.2 -relsizediff 0.1 -
663 relshift 0.1. Parameters were chosen in order to merge slightly differing representations of
664 alleles that were putatively identical from a biological point of view while preserving true allele
665 diversity at a given position.

666

667 SVs discovered from Oxford Nanopore data were also merged across samples using SVmerge
668 with the same parameters as described above. However, for Oxford Nanopore variants, we
669 modified SVmerge's default behavior which selects an allele randomly from a given SV cluster.
670 Instead, we forced the random selection to be made among the alleles that had been refined by

671 the SV refinement pipeline, if any, to favor those alleles whose representation was hopefully
672 closer to biological reality.

673

674 For the last batch combining Illumina and Oxford Nanopore variants, the two datasets described
675 above were merged using SVmerge. The default behaviour of SVmerge was again overridden
676 by systematically sampling among the alleles found by Illumina whenever a SV cluster
677 contained alleles found by both Illumina and Oxford Nanopore. Despite the greater power of
678 Oxford Nanopore data in discovering SVs, our reasoning was that if a variant was discovered by
679 both sequencing technologies, then the Illumina data was likely more precise given its higher
680 basecalling accuracy.

681

682 The methods used for genotyping were identical for all three batches. We prepared the VCF
683 files for input to Paragraph by removing variants located less than 1 kb away from chromosome
684 ends and padding the allele representations as required by Paragraph. We genotyped the 102
685 Illumina samples aligned by bwa mem following the recommendations outlined by Paragraph for
686 population-scale genotyping, i.e. the variants were genotyped independently for each sample
687 with multigrmpy, setting the -M option to 20 times the average sequencing depth for the sample.

688

689 We compared the genotyping results of the three batches against the Oxford Nanopore SV set
690 in order to assess genotyping sensitivity and precision. For this analysis, the set of variants
691 called from the Oxford Nanopore data by Sniffles and subsequently refined was considered to
692 be the ground truth. Structural variation calls made from Oxford Nanopore data may also be
693 erroneous, especially for smaller variants [2], so this approach of treating Oxford Nanopore
694 dataset as the ground truth is necessarily imperfect but nevertheless provides a good
695 comparison basis for our purposes.

696

697 We compared the SV genotype calls to the ground truth set using the R package *sveval* v. 2.0.0
698 [30]. For each of the 17 samples for which Oxford Nanopore data was available, we compared
699 the genotype calls made by Paragraph to the SVs identified in the Oxford Nanopore data for
700 that sample. SVs genotyped as homozygous for the alternate allele by Paragraph and present
701 in the Nanopore set were considered true positives, while SVs genotyped as homozygous for
702 the alternate allele by Paragraph but absent from the Nanopore set were considered false
703 positives. Note that, for benchmarking purposes, we essentially ignored heterozygous genotype
704 calls made by Paragraph since the truth set only contained homozygous calls as expected for
705 inbred lines. Sensitivity was defined as the ratio of the number of true positive calls to the total
706 number of SVs in the truth set, and precision as the ratio of the number of true positive calls to
707 the sum of true and false positive calls. We computed sample-wise precision-recall curves for
708 various SV size classes and SV types by using a range of read count thresholds (number of
709 reads required to support a genotype call) to filter the Paragraph genotype calls. We required
710 *sveval* to explicitly compare insertion sequences by setting *ins.seq.comp* = TRUE, but we
711 otherwise used default settings. We extended *sveval*'s functionality by also assessing
712 duplications under the same overlap conditions as the package already provides for deletions
713 and inversions. Benchmarks were performed both on the complete set of SVs and on a subset
714 of SVs located in non-repeat regions. A SV was defined as belonging to a repetitive region if it
715 had a 20% or higher overlap to regions in the repeat annotation for the Williams82 assembly
716 version 4 retrieved from Phytozome [66].

717
718 For the SVs discovered by Illumina, we computed additional precision-recall curves by filtering
719 the SVs in the dataset genotyped by Paragraph based on two different metrics of SV quality: (1)
720 the number of times the alternate allele is observed in homozygous genotype calls across the
721 whole population (referred to hereafter as the homozygous ALT count) and (2) the number of
722 calling tools (out of a maximum of four) that originally reported the SV. The more stringent

723 homozygous ALT count was used instead of alternate allele frequency as a measure of the
724 frequency of the SV in the population since true SVs are expected to be homozygous for the
725 alternate allele in these inbred lines. Note that both of these quality measures (homozygous
726 ALT count and the number of tools supporting an SV) effectively filter SV records and not
727 individual genotype calls. The objective of these analyses was to see whether filtering on SV
728 frequency or calling-tool support for variants could result in a higher quality dataset.

729

730 **Population structure**

731 We used the set of merged Illumina and Oxford Nanopore SVs genotyped by Paragraph to
732 evaluate whether SV calls could replicate population structure analyses made from SNV calls.
733 We applied methods similar to Torkamaneh et al. [6] in order to compute population structure for
734 the 102-sample population. We called SNVs using Platypus v. 0.8.1.1 [67] with parameters --
735 minMapQual=20 --minBaseQual=20 --maxVariants=10 --filterReadsWithUnmappedMates=0 --
736 filterReadsWithDistantMates=0 --filterReadPairsWithSmallInserts=0. We filtered Platypus calls
737 to keep only biallelic SNVs located on any of the 20 reference chromosomes. We only retained
738 SNVs with a minor allele frequency ≥ 0.05 , proportion of missing sites ≤ 0.4 , and heterozygosity
739 rate ≤ 0.1 . The resulting 1.27 M SNVs were converted to PLINK BED format [68] and used as
740 input to fastStructure v. 1.0 [69] using $k = 5$ as determined by Torkamaneh et al. [6]. A PCA was
741 computed on those SNVs using PLINK v1.90b5.3 with default parameters. A PCA was also
742 computed on the population-scale dataset of Illumina/Oxford Nanopore SVs genotyped with
743 Paragraph. For this analysis, we filtered SV genotype calls by setting those with less than two
744 supporting reads to missing. We also removed duplications, inversions, as well as records with
745 a homozygous ALT count < 4 or a proportion of missing sites ≥ 0.4 .

746

747 **Potential impact on genes**

748 We annotated deletions and insertions based on their overlap with various gene features. We

749 retrieved the positions of the gene models for Williams82 assembly 4 from Phytozome [66] and
750 determined for each SV whether it overlapped any of the following genic features: coding
751 sequences, non-coding genic sequences, and regions 5 kb upstream of genes. These
752 categories were mutually exclusive, such that an SV overlapping both coding and non-coding
753 sequences was only labeled as “coding sequences”. Similarly, an SV was only labeled as “5 kb
754 upstream” if it did not overlap any genic sequences. The SVs that overlapped none of the
755 features described above were labeled as “intergenic”.

756

757 We first used these annotations to assess whether SVs were over- or underrepresented within
758 particular genic features by comparing the observed proportions of deletions and insertions
759 overlapping each feature to what would be expected by chance. We used three different
760 measures of random expectation of the proportion of SVs overlapping genic features. The first
761 measure was a naive comparison to the proportion of the genome corresponding to each genic
762 feature. This comparison is however biased because repetitive regions (which are largely non-
763 genic) are less effectively queried for SVs than non-repetitive genic regions. Therefore, we also
764 replicated the analysis by excluding repeated regions, which provided a second measure of
765 random expectation. Finally, we performed a randomization test by estimating the distribution
766 over the proportions of SVs that would be expected to overlap each genic feature by random
767 chance. This was done by shuffling the start positions of SVs within the 100-kb genome-tiling
768 bins in which they are located 5,000 times and annotating them with the genic features
769 overlapped. We used 100-kb bins tiled along the whole genome instead of shuffling the
770 positions genome-wide to take into consideration the heterogeneity of the genome while
771 allowing SVs to be repositioned in a gene-agnostic manner.

772

773 We also used the genic feature annotations to study differences in mean alternate allele
774 frequencies of SVs depending on the features they overlapped. We averaged the frequencies of

775 insertions and deletions overlapping each of the four genic features and computed the
776 difference between the mean SV frequencies for each of the six possible pairwise combinations
777 of features. SVs with a frequency of 1 in the population were excluded from this analysis
778 because they might be due to errors in the reference assembly. Statistical significance was
779 assessed using a randomization test by shuffling the genic feature annotations 10,000 times to
780 get a distribution of mean SV frequency differences between feature groups under a random
781 scenario. We computed one-sided *p*-values by comparing the observed values to the random
782 distributions thus generated, using a significance threshold of $\alpha = 0.05 / 6 = 0.0083$ to
783 compensate for multiple testing.

784

785 Finally, we carried out enrichment analyses of GO [70] Biological Process terms and PFAM
786 domains [71] to assess whether high-frequency gene-impacting SVs were associated with
787 particular biological functions. We identified insertions and deletions with an alternate allele
788 frequency ≥ 0.5 and < 1 among those overlapping coding sequences and found 546 genes
789 overlapped by such SVs. These genes constituted our gene set of interest for the enrichment
790 analyses. We used the GOstats Bioconductor package v. 2.56.0 [72] along with GO and PFAM
791 annotations for Williams82 assembly version 4 retrieved from Soybase on April 20 2021 to test
792 this gene set for over- and underrepresentation of particular GO Biological Process terms or
793 PFAM protein domains. We only tested GO terms and PFAM domains that were represented by
794 at least 20 and 10 genes, respectively. For the GO terms, we used the conditional test as
795 implemented in GOstats and the GO.db annotation package v. 3.12.1 [73]. We applied a
796 Bonferroni correction to the *p*-values of both the GO and PFAM enrichment tests by multiplying
797 the *p*-values by the number of terms/domains tested.

798

799 **Transposable elements**

800 We annotated TEs in the SVs discovered using the SoyTEdb database [74] downloaded from
801 SoyBase [50]. We queried the deleted or inserted sequences of all deletions and insertions \geq
802 100 bp against SoyTEdb using blastn v. 2.11.0+ [75] with default parameters. Any queried
803 sequence that aligned to a TE in the database with at least 80% of the query length and 80% of
804 the length of the TE sequence was considered a match and annotated accordingly with the
805 classification of the best-matching TE. All alignments that matched these criteria had an
806 extremely small E-value ($< 10^{-80}$) and therefore no additional filtering on this was needed.

807

808 The annotated SVs were then used to determine both the proportion of polymorphic TEs
809 belonging to each category and the physical location of polymorphic TEs in the genome. We
810 also computed the proportions of TEs ≥ 100 bp in each category within the reference repeat
811 annotation from Phytozome and compared those to the estimated proportions in the SV dataset.
812 The estimated number of polymorphic TEs within various LTR-retrotransposon families and
813 DNA TE types were also compared to the number of non-reference TEs found by Tian et al. [37]
814 to check whether our results were consistent with previous reports.

815

816 Soybean DNA TEs have received little attention compared to retrotransposons, which are more
817 prevalent and polymorphic in this species [37, e.g. 76]. DNA TEs that have TIR typically
818 transpose using a “cut and paste” mechanism. This mechanism generates a TSD upon insertion
819 into the genome, and leaves this TSD as well as possible additional nucleotides upon excision
820 due to DNA repair [77]. In order to study the dynamics of polymorphic DNA TEs within our
821 population, we devised a pipeline based on local assembly and multiple sequence alignment of
822 the DNA TE insertions. Briefly, the pipeline locally assembles Oxford Nanopore reads
823 surrounding the sites of polymorphic DNA TEs for all samples using wtdbg2 and aligns these
824 assemblies to each other using MAFFT v. 7.475 [78] before identifying TIR and TSD sequences
825 with Generic Repeat Finder v. 1.0 [79]. For more details on the pipeline, see Supplemental

826 Methods (Additional file 1). Our goal with this pipeline was to determine whether the
827 insertion/deletion polymorphisms at various sites were due to novel TE insertion, TE excision, or
828 a combination of both phenomena. We applied this pipeline to SVs that were annotated as TIR
829 DNA TEs and whose matching sequence in the SoyTEdb database was matched by at least
830 three SVs. We limited ourselves to TE sequences that were matched by at least three SV
831 events under the assumption that TEs present in multiple copies were more likely to have been
832 recently active. For insertions that had both TIR and TSD sequences unambiguously identified,
833 we computed the proportion of matching nucleotides in the alignment of the two terminal
834 repeats and averaged the values across all local assemblies bearing the insertion in order to get
835 a single value for that SV.

836

837 **Software used**

838 Unless otherwise stated, all statistical analyses and data manipulation were conducted in R
839 version 3.5.0 or 4.0.3 [80] and Bioconductor version 3.08 or 3.12 [81]. Analyses made use of
840 Bioconductor packages Biostrings v. 2.58.0 [82], GenomicRanges v. 1.42.0 [83], Rsamtools v.
841 2.6.0 [84], rtracklayer v. 1.50.0 [85] and VariantAnnotation v. 1.36.0 [86]. All scripts used for the
842 analyses described in this paper are available on GitHub [87].

843

844 **Additional files**

845 Additional file 1: Supplemental methods, supplemental tables S1 to S9 and supplemental
846 figures S1 to S21 (PDF 12 MB)

847

848 Additional file 2: Statistics of the conditional hypergeometric test for the overrepresentation of
849 GO Biological Process terms using the GOstats R package. P-values are Bonferroni-corrected
850 p-values. (CSV 141 KB)

851

852 Additional file 3: Statistics of the conditional hypergeometric test for the underrepresentation of
853 GO Biological Process terms using the GOstats R package. P-values are Bonferroni-corrected
854 p-values. (CSV 265 KB)

855

856 Additional file 4: Statistics of the hypergeometric test for the overrepresentation of PFAM
857 domains using the GOstats R package. P-values are Bonferroni-corrected p-values. (CSV 18
858 KB)

859

860 Additional file 5: Statistics of the hypergeometric test for the underrepresentation of PFAM
861 domains using the GOstats R package. P-values are Bonferroni-corrected p-values. (CSV 95
862 KB)

863

864 Additional file 6: SVs identified as polymorphic transposable elements among the dataset of
865 combined Illumina/Oxford Nanopore variants genotyped with Paragraph. Positions of the SVs
866 and metadata about their best blastn match in the SoyTEdb database are described. (CSV 598
867 KB)

868

869 Additional file 7: Proportion of matching nucleotides in TIR of SVs for which intact TSD
870 sequences and matching TIR were identified with GenericRepeatFinder (CSV 2.4 KB).

871

872 Additional file 8: Multiple alignment of the Williams82 assembly version 4 reference sequence
873 and local *de novo* assemblies of 7 samples at the site of a 480-bp Stowaway MITE insertion
874 (Gm04:2,257,090). Samples OAC Petrel and Roland bear the 480-bp insertion, while Alta bears
875 the 6-bp TACGAG insertion; other samples match the reference sequence. Asterisks mark the
876 locations of the TSD sequences in samples OAC Petrel and Roland. (TXT 6.2 KB)

877

878 **Abbreviations**

879 GO: gene ontology; MITE: miniature inverted-repeat transposable element; PCA: principal
880 component analysis; SRA: sequence read archive; SV: structural variant; SNV: single-
881 nucleotide variant; TE: transposable element; TIR: terminal inverted repeat; TSD: target site
882 duplication

883

884 **Declarations**

885

886 **Ethics approval and consent to participate**

887 Not applicable.

888

889 **Consent for publication**

890 Not applicable.

891

892 **Availability of data and materials**

893 The Illumina sequencing data used in this study is available on the SRA repository through
894 BioProject accession number PRJNA356132 [46]. The Oxford Nanopore sequencing data
895 generated during the current study is available in the SRA repository through BioProject
896 accession number PRJNA751911 [88].

897

898 The SoyTEDb database is available on SoyBase [89].

899 Gene Ontology annotations for Williams82 assembly version 4 [90] as well as chloroplast and
900 mitochondrion genome sequences [91] are also available on SoyBase.

901

902 The non-reference transposable elements found by Tian et al. (2012) can be downloaded from
903 the supplementary data to their paper [37].

904

905 The reference genome sequence and annotation of soybean cultivar Williams82, assembly
906 version 4, are available on Phytozome [92].

907

908 VCF files generated during this study and results of the permutation test for the analysis of the
909 proportion of SVs overlapping various genic features are available on the figshare repository
910 [93].

911

912 The code for all the analyses described in the paper [87] and the breakpoint refinement pipeline
913 [94] are available on GitHub. Versions of the code at the time of submission are archived on the
914 figshare repository for the breakpoint refinement pipeline [95] and the analysis code [96].

915

916 **Competing interests**

917 The authors declare that they have no competing interests.

918

919 **Funding**

920 This work was supported by the SoyaGen grant (www.soyagen.ca) awarded to F. Belzile and
921 funded by Génome Québec, Genome Canada, the government of Canada, the Ministère de
922 l'Économie, Science et Innovation du Québec, Semences Program Inc., Syngenta Canada Inc.,
923 Sevita Genetics, Coop Fédérée, Grain Farmers of Ontario, Saskatchewan Pulse Growers,
924 Manitoba Pulse & Soybean Growers, the Canadian Field Crop Research Alliance and
925 Producteurs de grains du Québec. M-A. Lemay has been supported by a NSERC Canada

926 Vanier Graduate Scholarship, a FRQNT doctoral B2X scholarship, a NSERC Michael Smith
927 Foreign Study Supplement, and a scholarship from the AgroPhytoSciences NSERC CREATE
928 Training Program. J. A. Sibbesen was supported by the Carlsberg Foundation. None of the
929 funding bodies were involved in study design, data acquisition, data analysis, interpretation of
930 the results, or manuscript writing.

931

932 **Authors' contributions**

933 Conception and design of the study: MAL, JAS, DT, FB. Illumina sequencing: DT. Oxford
934 Nanopore sequencing: MAL, JH, RCL. Data analysis: MAL. Data interpretation: MAL, JAS, FB.
935 Manuscript drafting: MAL, JAS, FB. All authors have revised the manuscript and approved its
936 submission.

937

938 **Acknowledgements**

939 The authors thank Brian Boyle for assistance with Oxford Nanopore sequencing, Maxime de
940 Ronne for providing the CTAB protocol, Anders Krogh for hosting MAL at the University of
941 Copenhagen, Claire Mérot for providing comments on the manuscript, Malcolm Morrison for
942 providing some of the plant materials, as well as Dave Deandre Istanto and Matthew Hudson for
943 providing access to unpublished data on soybean polymorphic transposable elements. None of
944 the funding bodies were involved in study design, data acquisition, data analysis, interpretation
945 of the results, or manuscript writing.

946

947

948

949

950

951 **Tables**

952 **Table 1:** Number of SVs called from the Illumina data per calling tool, SV type and size class.

Calling program	[50bp – 100bp[[100bp – 1kb[[1kb – 10kb[≥ 10kb ^a		
	DEL ^b	INS ^c	DUP ^d	INV ^e	DEL	INS	DUP	INV	DEL	INS	DUP	INV	DEL	DUP	INV
asmvar	11018	3575	0	0	14877	2243	0	0	5748	1	0	0	4681	0	0
manta	9664	3358	453	0	12378	1815	3114	0	11463	0	4448	0	7325	5034	0
smoove	4168	0	22	45	6489	0	1208	149	4687	0	981	33	1794	975	47
svaba	7288	2284	673	21	6907	215	16081	292	2969	0	1548	190	512	458	223
merged ^f	17199	5023	656	61	22980	3165	9810	296	13007	1	4316	135	10640	4696	178

^a Insertions ≥ 10kb are not shown because none were called

^b DEL: deletions,

^c INS: insertions

^d DUP: duplications

^e INV: inversions

^f merged: the dataset merged using SVmerge

954 **Table 2:** Number and span of polymorphic and reference transposable elements of different

955 types.

TE type	REF ^a (%)		DEL ^b (%)		INS ^c (%)	
	N ^d	Mb ^e	N	kb ^f	N	kb
Copia LTR retrotransposons	91241 (35.1)	170 (43.0)	1154 (44.6)	5594 (43.8)	1303 (54.5)	6692 (63.1)
Gypsy LTR retrotransposons	71390 (27.5)	139 (35.2)	949 (36.7)	5745 (45)	718 (30)	2949 (27.8)
Non-LTR retrotransposons	8078 (3.1)	10 (2.5)	144 (5.6)	449 (3.5)	99 (4.1)	307 (2.9)
DNA TE	89300 (34.3)	76 (19.2)	339 (13.1)	989 (7.7)	271 (11.3)	654 (6.2)

^a REF: transposable elements ≥ 100 bp in the reference genome

^b DEL: deletions relative to the reference that are annotated as TEs

^c INS: insertions relative to the reference that are annotated as TEs

^d N: Number of reference elements, deletions or insertions matching given TE type

^e Mb: Total length of reference elements of a given type, in Mb

^f kb: Total length of polymorphic elements matching given TE type, in kb

957

958

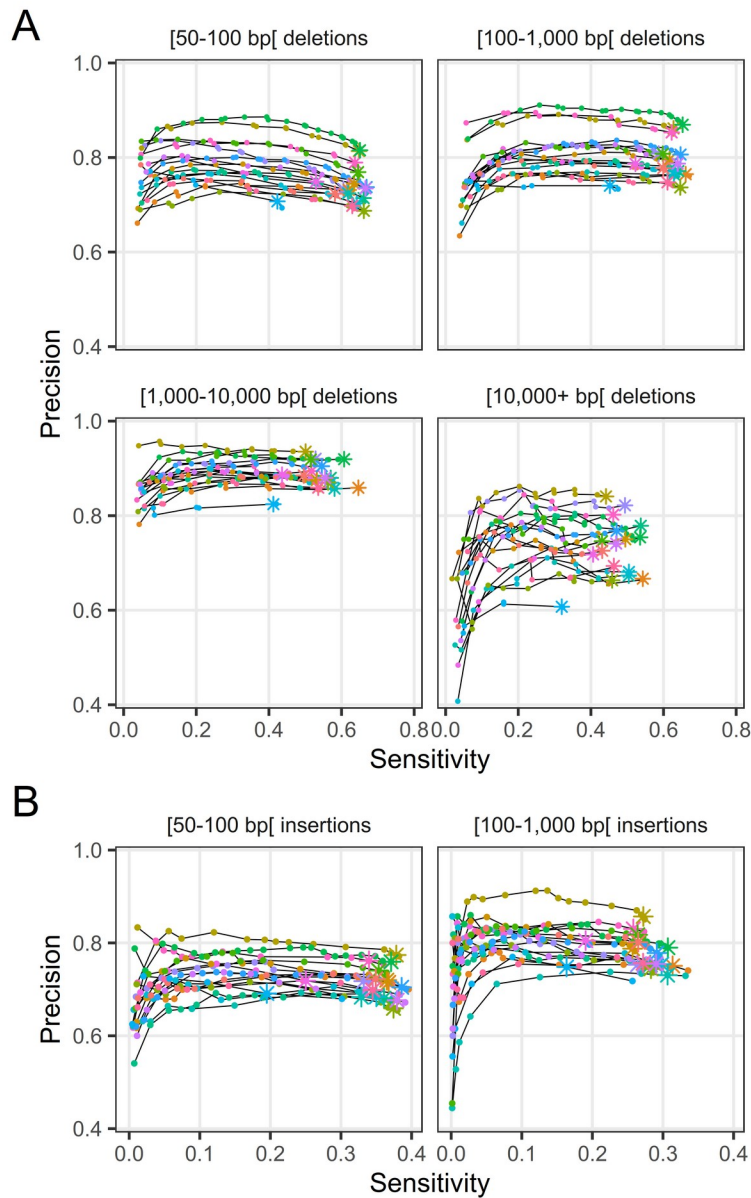
959

960

961

962

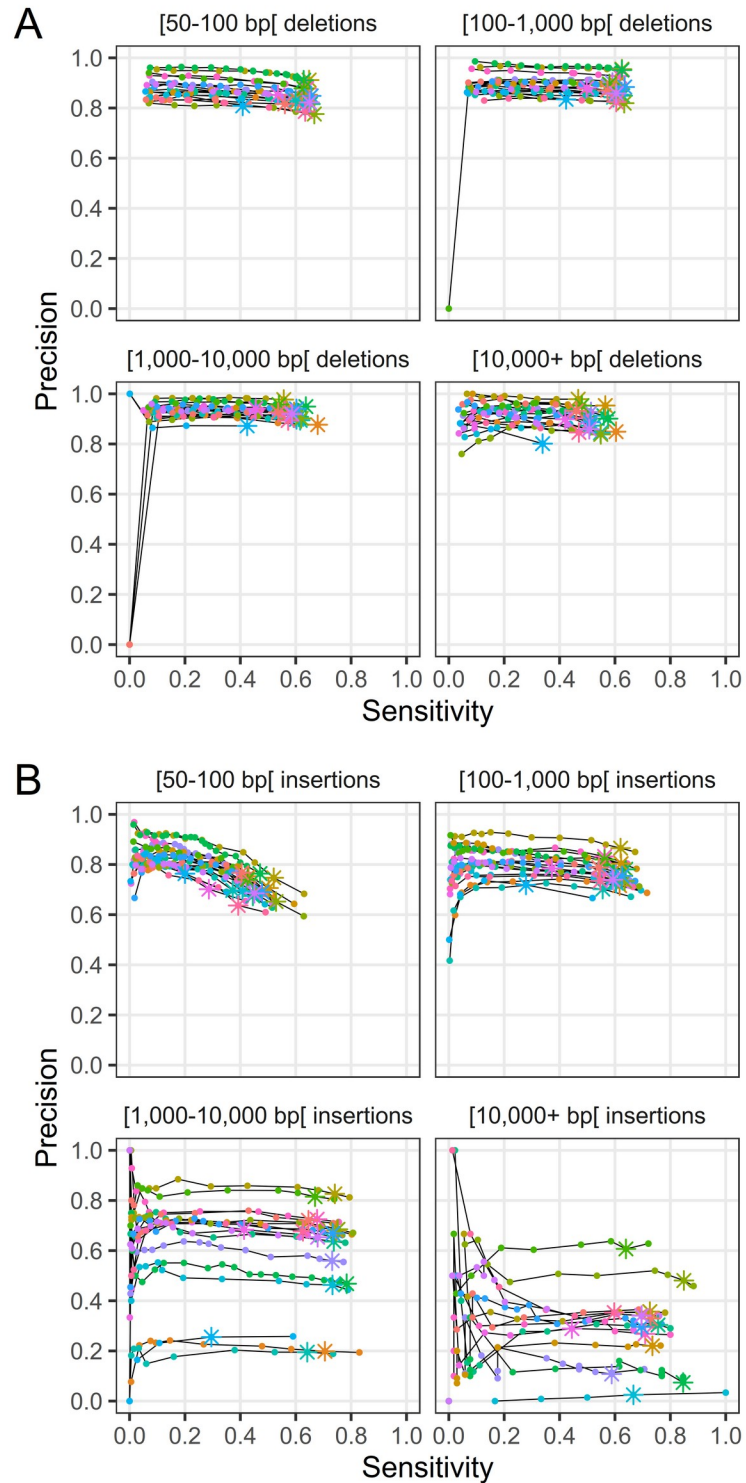
963 **Figures**



964 **Figure 1:** Genotyping sensitivity and precision of (A) deletions and (B) insertions discovered
965 from the Illumina data. Each line and color represents one of 17 samples. The different plots
966 correspond to different SV lengths. The points correspond to different filtering thresholds on the
967 minimum number of Illumina reads required to support a genotype call. The asterisks indicate a
968 minimum number of supporting reads of 2; points to the left of these for a given line represent

969 increasingly stringent filtering threshold values (i.e. a greater number of reads supporting a
970 genotype call).

971

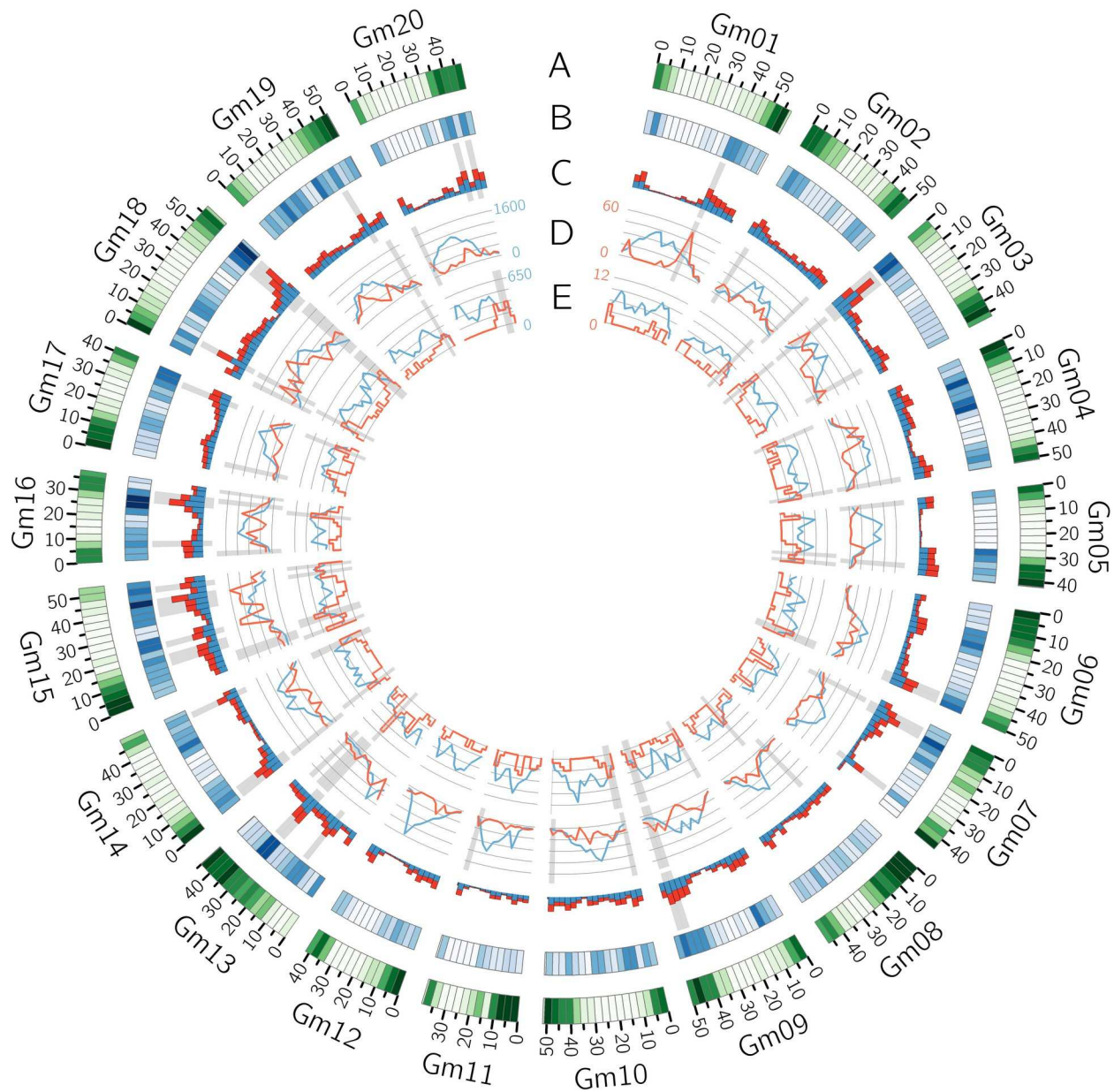


973 **Figure 2:** Genotyping sensitivity and precision of (A) deletions and (B) insertions discovered
974 from the Oxford Nanopore data. Each line and color represents one of 17 samples. The different

975 plots correspond to different SV lengths. The points correspond to different filtering thresholds
976 on the minimum number of Illumina reads required to support a genotype call. The asterisks
977 indicate a minimum number of supporting reads of 2; points to the left of these for a given line
978 represent increasingly stringent filtering threshold values (i.e. a greater number of reads
979 supporting a genotype call).

980

981



983 **Figure 3:** Circos plot of the distribution of various features within 3-Mb bins along the reference
984 assembly version 4 of Williams82. (A) Gene density (B) Density of SNVs called by Platypus (C)
985 Number of deletions (blue) and insertions (red) discovered within each bin. The bins with the
986 10% highest SV density (insertions and deletions considered together) are highlighted in gray.
987 (D) Number of reference (blue) and polymorphic (red) LTR Copia and LTR Gypsy elements
988 (summed together). (E) Number of reference (blue) and polymorphic (red) DNA transposable

989 elements. The gray highlights in tracks D and E show the bins with the 10% highest
990 polymorphic/reference ratios.

991

992

993

994

995

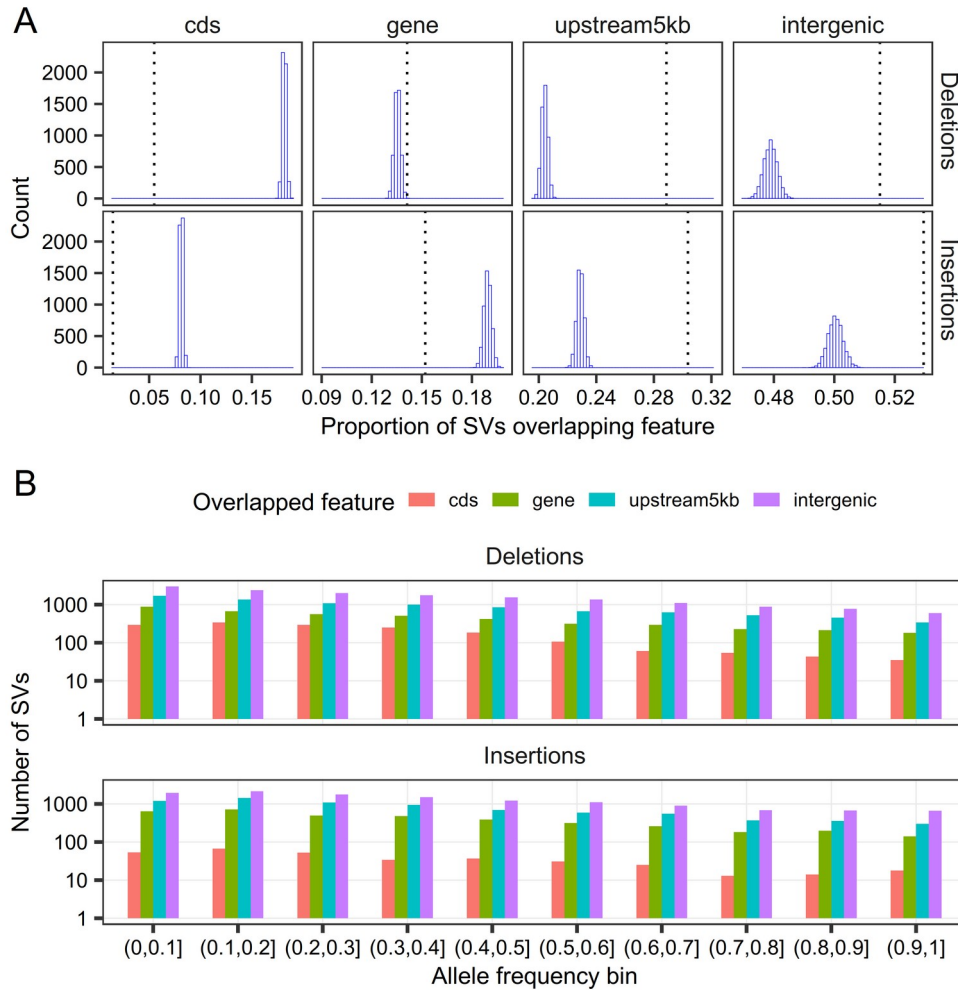
996

997

998

999

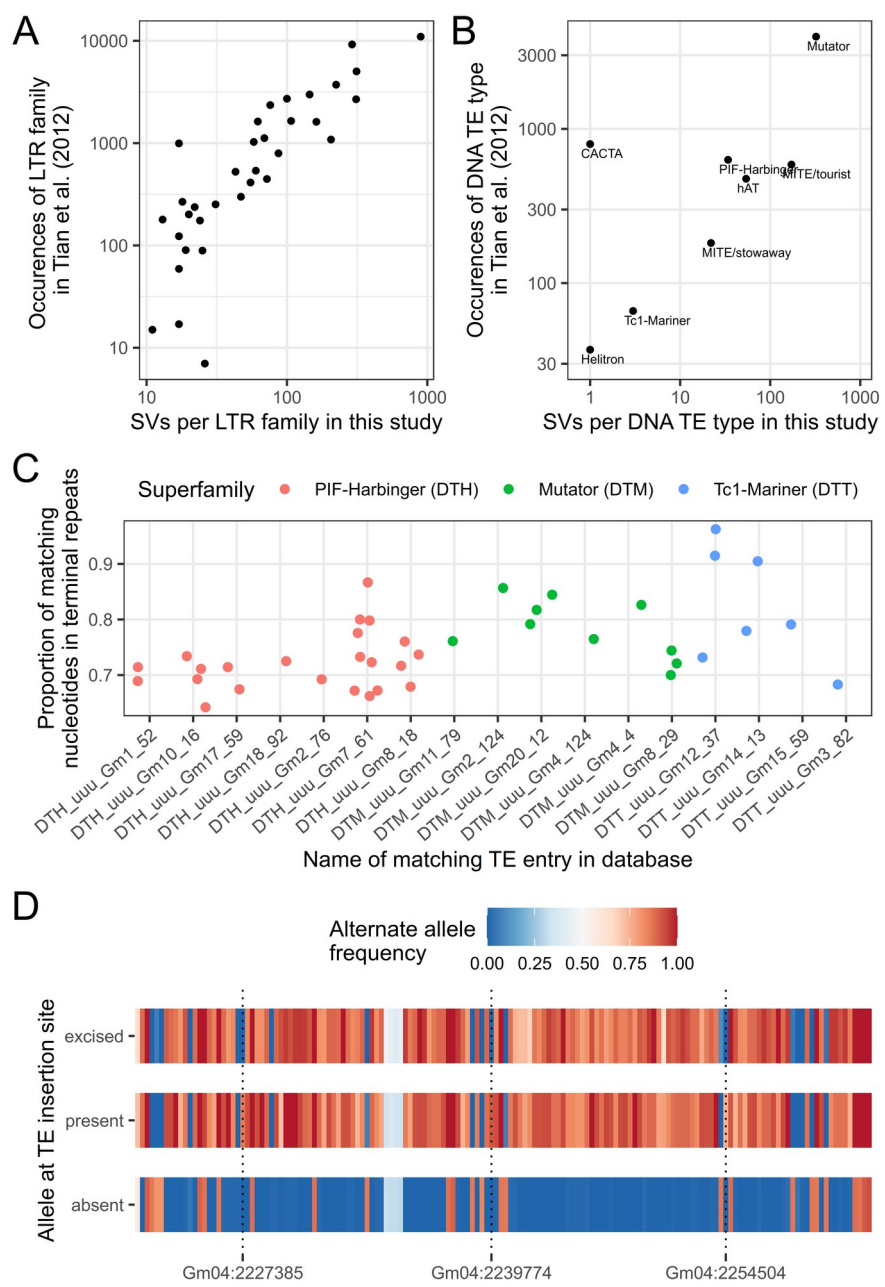
1000



1002 **Figure 4:** Analysis of the overlap of SVs with gene models. (A) Distributions of the proportions
1003 of deletions and insertions overlapping various genic features as generated by a randomization
1004 test (5,000 iterations). Observed proportions for each SV type and genic feature are indicated
1005 by a vertical dotted line. One-sided p-values are $< 2 \times 10^{-4}$ for all comparisons except for
1006 deletions overlapping genes, for which the p-value is 4×10^{-4} . (B) Distribution of the allele
1007 frequencies of deletions and insertions depending on the genic features they overlap. Note the
1008 logarithmic scale on the y-axis. cds: SVs overlapping coding sequences; gene: SVs overlapping
1009 non-coding genic sequences; upstream5kb: SVs overlapping regions 5 kb upstream of genes,
1010 but not any genic sequences; intergenic: SVs that do not overlap any of the other features.

1011

1012



1014 **Figure 5:** Analysis of the polymorphic TEs found in this study. Comparison of the number of
1015 polymorphic TEs per (A) LTR family and (B) DNA TE type found in Tian et al. [37] and in this

1015 study. Differences in y- and x-scales are partly explained by the fact that counts for Tian et al.
1016 are summed over occurrences in all samples whereas our data counts each SV only once. Note
1017 that all scales are logarithmic. (C) Proportion of matching nucleotides between the two terminal
1018 repeats for TE sequences corresponding to 40 different SVs grouped by DNA TE superfamily
1019 and by the identifier of the TE sequence they matched in the SoyTEdb database. (D) Alternate
1020 allele frequencies of 156 SNVs located in a ~39-kb linkage disequilibrium block between
1021 positions Gm04:2,220,398 and Gm04:2,259,326. Frequencies were computed for three different
1022 groups of samples depending on their genotype at the TE insertion site (Gm04:2,257,090).
1023 absent: absence of the TE insertion, which corresponds to the reference allele (71 samples);
1024 present: presence of the 480-bp Stowaway MITE (9 samples); excised: presence of a 6-bp
1025 insertion at the insertion site, putatively left by excision of the TE insertion (14 samples). The
1026 locations of three SNVs whose frequency in the “present” and “excised” groups diverge are
1027 shown with dotted vertical lines.

1028

1029 **References**

- 1030 1. Bayer PE, Golicz AA, Scheben A, Batley J, Edwards D. Plant pan-genomes are the new
1031 reference. *Nat Plants*. 2020;6:914–20. doi:10.1038/s41477-020-0733-0.
- 1032 2. Ho SS, Urban AE, Mills RE. Structural variation in the sequencing era. *Nat Rev Genet*.
1033 2020;21:171–89. doi:10.1038/s41576-019-0180-9.
- 1034 3. Marroni F, Pinochio S, Morgante M. Structural variation and genome complexity: Is
1035 dispensable really dispensable? *Curr Opin Plant Biol*. 2014;18:31–6.
1036 doi:10.1016/j.pbi.2014.01.003.
- 1037 4. Yue J-X, Li J, Aigrain L, Hallin J, Persson K, Oliver K, et al. Contrasting evolutionary genome
1038 dynamics between domesticated and wild yeasts. *Nat Genet*. 2017;49:913–24.

1039 doi:10.1038/ng.3847.

1040 5. Catanach A, Crowhurst R, Deng C, David C, Bernatchez L, Wellenreuther M. The genomic
1041 pool of standing structural variation outnumbers single nucleotide polymorphism by threefold in
1042 the marine teleost *Chrysophrys auratus*. *Mol Ecol*. 2019;28:1210–23. doi:10.1111/mec.15051.

1043 6. Torkamaneh D, Laroche J, Tardivel A, O'Donoughue L, Cober E, Rajcan I, et al.
1044 Comprehensive description of genomewide nucleotide and structural variation in short-season
1045 soya bean. *Plant Biotechnol J*. 2018;16:749–59. doi:10.1111/pbi.12825.

1046 7. Weischenfeldt J, Symmons O, Spitz F, Korbel JO. Phenotypic impact of genomic structural
1047 variation: insights from and for human disease. *Nat Rev Genet*. 2013;14:125–38.
1048 doi:10.1038/nrg3373.

1049 8. Carvalho CMB, Lupski JR. Mechanisms underlying structural variant formation in genomic
1050 disorders. *Nat Rev Genet*. 2016;17:224–38. doi:10.1038/nrg.2015.25.

1051 9. Cook DE, Lee TG, Guo X, Melito S, Wang K, Bayless AM, et al. Copy Number Variation of
1052 Multiple Genes at Rhg1 Mediates Nematode Resistance in Soybean. *Science*. 2012;338:1206–
1053 9. doi:10.1126/science.1228746.

1054 10. Maron LG, Guimaraes CT, Kirst M, Albert PS, Birchler JA, Bradbury PJ, et al. Aluminum
1055 tolerance in maize is associated with higher MATE1 gene copy number. *Proc Natl Acad Sci*.
1056 2013;110:5241–6. doi:10.1073/pnas.1220766110.

1057 11. Studer A, Zhao Q, Ross-Ibarra J, Doebley J. Identification of a functional transposon
1058 insertion in the maize domestication gene tb1. *Nat Genet*. 2011;43:1160–3. doi:10.1038/ng.942.

1059 12. Alonge M, Wang X, Benoit M, Soyk S, Pereira L, Zhang L, et al. Major Impacts of
1060 Widespread Structural Variation on Gene Expression and Crop Improvement in Tomato. *Cell*.
1061 2020;182:145–161.e23. doi:10.1016/j.cell.2020.05.021.

1062 13. Su Z, Bernardo A, Tian B, Chen H, Wang S, Ma H, et al. A deletion mutation in TaHRC
1063 confers Fhb1 resistance to Fusarium head blight in wheat. *Nat Genet.* 2019;51:1099–105.
1064 doi:10.1038/s41588-019-0425-8.

1065 14. Qian L, Voss-Fels K, Cui Y, Jan HU, Samans B, Obermeier C, et al. Deletion of a Stay-
1066 Green Gene Associates with Adaptive Selection in *Brassica napus*. *Mol Plant.* 2016;9:1559–69.
1067 doi:10.1016/j.molp.2016.10.017.

1068 15. Mérot C, Oomen RA, Tigano A, Wellenreuther M. A Roadmap for Understanding the
1069 Evolutionary Significance of Structural Genomic Variation. *Trends Ecol Evol.* 2020;35:561–72.
1070 doi:10.1016/j.tree.2020.03.002.

1071 16. Alkan C, Coe BP, Eichler EE. Genome structural variation discovery and genotyping. *Nat*
1072 *Rev Genet.* 2011;12:363–76. doi:10.1038/nrg2958.

1073 17. Saxena RK, Edwards D, Varshney RK. Structural variations in plant genomes. *Brief Funct*
1074 *Genomics.* 2014;13:296–307. doi:10.1093/bfgp/elu016.

1075 18. Cameron DL, Di Stefano L, Papenfuss AT. Comprehensive evaluation and characterisation
1076 of short read general-purpose structural variant calling software. *Nat Commun.* 2019;10:3240.
1077 doi:10.1038/s41467-019-11146-4.

1078 19. Chaisson MJP, Sanders AD, Zhao X, Malhotra A, Porubsky D, Rausch T, et al. Multi-
1079 platform discovery of haplotype-resolved structural variation in human genomes. *Nat Commun.*
1080 2019;10. doi:10.1287/opre.42.6.1042.

1081 20. Kosugi S, Momozawa Y, Liu X, Terao C, Kubo M, Kamatani Y. Comprehensive evaluation of
1082 structural variation detection algorithms for whole genome sequencing. *Genome Biol.*
1083 2019;20:117. doi:10.1186/s13059-019-1720-5.

1084 21. Sedlazeck FJ, Lee H, Darby CA, Schatz MC. Piercing the dark matter: Bioinformatics of

1085 1086 long-range sequencing and mapping. *Nat Rev Genet.* 2018;19:329–46. doi:10.1038/s41576-018-0003-4.

1087 1088 22. Cretu Stancu M, Van Roosmalen MJ, Renkens I, Nieboer MM, Middelkamp S, De Ligt J, et al. Mapping and phasing of structural variation in patient genomes using nanopore sequencing.

1089 *Nat Commun.* 2017;8:1–13. doi:10.1038/s41467-017-01343-4.

1090 23. Heller D, Vingron M. SVIM: structural variant identification using mapped long reads. *Bioinformatics.* 2019;35:2907–15. doi:10.1093/bioinformatics/btz041.

1091 1092 24. Sedlazeck FJ, Rescheneder P, Smolka M, Fang H, Nattestad M, von Haeseler A, et al. Accurate detection of complex structural variations using single-molecule sequencing. *Nat Methods.* 2018;15:461–8. doi:10.1038/s41592-018-0001-7.

1093 1094 1095 25. Tham CY, Tirado-Magallanes R, Goh Y, Fullwood MJ, Koh BTH, Wang W, et al. NanoVar: accurate characterization of patients' genomic structural variants using low-depth nanopore sequencing. *Genome Biol.* 2020;21:56. doi:10.1186/s13059-020-01968-7.

1096 1097 1098 26. De Coster W, De Rijk P, De Roeck A, De Pooter T, D'Hert S, Strazisar M, et al. Structural variants identified by Oxford Nanopore PromethION sequencing of the human genome. *Genome Res.* 2019;29:1178–87. doi:10.1101/434118.

1099 1100 1101 27. Choi JY, Lye ZN, Groen SC, Dai X, Rughani P, Zaaijer S, et al. Nanopore sequencing-based genome assembly and evolutionary genomics of circum-basmati rice. *Genome Biol.* 2020;21:21. doi:10.1186/s13059-020-1938-2.

1102 1103 1104 28. Chawla HS, Lee H, Gabur I, Vollrath P, Tamilselvan-Nattar-Amutha S, Obermeier C, et al. Long-read sequencing reveals widespread intragenic structural variants in a recent allopolyploid crop plant. *Plant Biotechnol J.* 2021;19:240–50. doi:10.1111/pbi.13456.

1105 1106 1107 29. Chen S, Krusche P, Dolzhenko E, Sherman RM, Petrovski R, Schlesinger F, et al.

1108 1108 Paragraph: A graph-based structural variant genotyper for short-read sequence data. *Genome*
1109 *Biol.* 2019;20. doi:10.1101/635011.

1110 1110 30. Hickey G, Heller D, Monlong J, Sibbesen JA, Sirén J, Eizenga J, et al. Genotyping structural
1111 variants in pangenome graphs using the vg toolkit. *Genome Biol.* 2020;21:35.
1112 doi:10.1186/s13059-020-1941-7.

1113 1113 31. Sibbesen JA, Maretty L, The Danish Pan-Genome Consortium, Krogh A. Accurate
1114 genotyping across variant classes and lengths using variant graphs. *Nat Genet.* 2018;50:1054–
1115 9. doi:10.1038/s41588-018-0145-5.

1116 1116 32. Liu Y, Du H, Li P, Shen Y, Peng H, Liu S, et al. Pan-Genome of Wild and Cultivated
1117 Soybeans. *Cell.* 2020;182:162–176.e13. doi:10.1016/j.cell.2020.05.023.

1118 1118 33. Anderson JE, Kantar MB, Kono TY, Fu F, Stec AO, Song Q, et al. A Roadmap for
1119 Functional Structural Variants in the Soybean Genome. *G3 Genes|Genomes|Genetics.*
1120 2014;4:1307–18. doi:10.1534/g3.114.011551.

1121 1121 34. McHale LK, Haun WJ, Xu WW, Bhaskar PB, Anderson JE, Hyten DL, et al. Structural
1122 variants in the soybean genome localize to clusters of biotic stress-response genes. *Plant*
1123 *Physiol.* 2012;159:1295–308. doi:10.1104/pp.112.194605.

1124 1124 35. Maldonado dos Santos JV, Valliyodan B, Joshi T, Khan SM, Liu Y, Wang J, et al. Evaluation
1125 of genetic variation among Brazilian soybean cultivars through genome resequencing. *BMC*
1126 *Genomics.* 2016;17:1–18. doi:10.1186/s12864-016-2431-x.

1127 1127 36. Torkamaneh D, Lemay M-A, Belzile F. The pan-genome of the cultivated soybean (PanSoy)
1128 reveals an extraordinarily conserved gene content. *Plant Biotechnol J.* 2021;:pbi.13600.
1129 doi:10.1111/pbi.13600.

1130 1130 37. Tian Z, Zhao M, She M, Du J, Cannon SB, Liu X, et al. Genome-Wide Characterization of

1131 1131 Nonreference Transposons Reveals Evolutionary Propensities of Transposons in Soybean.

1132 1132 *Plant Cell.* 2012;24:4422–36. doi:10.1105/tpc.112.103630.

1133 1133 38. Shahid S, Slotkin RK. The current revolution in transposable element biology enabled by

1134 1134 long reads. *Curr Opin Plant Biol.* 2020;54:49–56. doi:10.1016/j.pbi.2019.12.012.

1135 1135 39. Domínguez M, Dugas E, Benchouaia M, Leduque B, Jiménez-Gómez JM, Colot V, et al.

1136 1136 The impact of transposable elements on tomato diversity. *Nat Commun.* 2020;11:4058.

1137 1137 doi:10.1038/s41467-020-17874-2.

1138 1138 40. Liu B, Kanazawa A, Matsumura H, Takahashi R, Harada K, Abe J. Genetic Redundancy in

1139 1139 Soybean Photoresponses Associated With Duplication of the Phytochrome A Gene. *Genetics.*

1140 1140 2008;180:995–1007. doi:10.1534/genetics.108.092742.

1141 1141 41. Sirén J, Monlong J, Chang X, Novak AM, Eizenga JM, Markello C, et al. Genotyping

1142 1142 common, large structural variations in 5,202 genomes using pangenomes, the Giraffe mapper,

1143 1143 and the vg toolkit. *bioRxiv.* 2021. Preprint at <https://doi.org/10.1101/2020.12.04.412486>.

1144 1144 42. Ebert P, Audano PA, Zhu Q, Rodriguez-Martin B, Porubsky D, Bonder MJ, et al. Haplotype-

1145 1145 resolved diverse human genomes and integrated analysis of structural variation. *Science.*

1146 1146 2021;372:eabf7117. doi:10.1126/science.abf7117.

1147 1147 43. Fuentes RR, Chebotarov D, Duitama J, Smith S, De la Hoz JF, Mohiyuddin M, et al.

1148 1148 Structural variants in 3000 rice genomes. *Genome Res.* 2019;29:870–80.

1149 1149 doi:10.1101/gr.241240.118.

1150 1150 44. Zhou Y, Minio A, Massonet M, Solares E, Lv Y, Beridze T, et al. The population genetics of

1151 1151 structural variants in grapevine domestication. *Nat Plants.* 2019;5:965–79. doi:10.1038/s41477-

1152 1152 019-0507-8.

1153 1153 45. Istanto DD. Whole genomic structural variant calling in soybean: analysis on 481 different

1154 soybean lines. University of Illinois at Urbana-Champaign; 2020.

1155 <https://www.ideals.illinois.edu/handle/2142/107902>.

1156 46. NCBI BioProject PRJNA356132. <https://www.ncbi.nlm.nih.gov/bioproject/?term=PRJNA356132>.

1158 47. Bushnell B. BBTools v. 38.25. sourceforge.net/projects/bbmap/.

1159 48. Li H, Durbin R. Fast and accurate short read alignment with Burrows-Wheeler transform.

1160 *Bioinformatics*. 2009;25:1754–60. doi:10.1093/bioinformatics/btp324.

1161 49. Valliyodan B, Cannon SB, Bayer PE, Shu S, Brown A V., Ren L, et al. Construction and

1162 comparison of three reference-quality genome assemblies for soybean. *Plant J.*

1163 2019;100:1066–82. doi:10.1111/tpj.14500.

1164 50. Grant D, Nelson RT, Cannon SB, Shoemaker RC. SoyBase, the USDA-ARS soybean

1165 genetics and genomics database. *Nucleic Acids Res.* 2010;38 suppl_1:D843–6.

1166 doi:10.1093/nar/gkp798.

1167 51. Li H, Handsaker B, Wysoker A, Fennell T, Ruan J, Homer N, et al. The Sequence

1168 Alignment/Map format and SAMtools. *Bioinformatics*. 2009;25:2078–9.

1169 doi:10.1093/bioinformatics/btp352.

1170 52. Garrison E. bamaddr. <https://github.com/ekg/bamaddr>.

1171 53. Liu S, Huang S, Rao J, Ye W, Krogh A, Wang J. Discovery, genotyping and characterization

1172 of structural variation and novel sequence at single nucleotide resolution from de novo genome

1173 assemblies on a population scale. *Gigascience*. 2015;4:64. doi:10.1186/s13742-015-0103-4.

1174 54. Chen X, Schulz-Trieglaff O, Shaw R, Barnes B, Schlesinger F, Källberg M, et al. Manta:

1175 rapid detection of structural variants and indels for germline and cancer sequencing

1176 applications. *Bioinformatics*. 2016;32:1220–2. doi:10.1093/bioinformatics/btv710.

1177 55. Wala JA, Bandopadhyay P, Greenwald NF, O'Rourke R, Sharpe T, Stewart C, et al.

1178 SvABA: genome-wide detection of structural variants and indels by local assembly. *Genome*
1179 *Res.* 2018;28:581–91. doi:10.1101/gr.221028.117.

1180 56. Layer RM, Chiang C, Quinlan AR, Hall IM. LUMPY: a probabilistic framework for structural
1181 variant discovery. *Genome Biol.* 2014;15:R84. doi:10.1186/gb-2014-15-6-r84.

1182 57. Pedersen BS, Quinlan AR. Duphold: scalable, depth-based annotation and curation of high-
1183 confidence structural variant calls. *Gigascience*. 2019;8:1–5. doi:10.1093/gigascience/giz040.

1184 58. Magoc T, Salzberg SL. FLASH: fast length adjustment of short reads to improve genome
1185 assemblies. *Bioinformatics*. 2011;27:2957–63. doi:10.1093/bioinformatics/btr507.

1186 59. Luo R, Liu B, Xie Y, Li Z, Huang W, Yuan J, et al. SOAPdenovo2: an empirically improved
1187 memory efficient short-read de novo assembler. *Gigascience*. 2012;1:18. doi:10.1186/2047-
1188 217X-1-18.

1189 60. Kielbasa SM, Wan R, Sato K, Horton P, Frith MC. Adaptive seeds tame genomic sequence
1190 comparison. *Genome Res.* 2011;21:487–93. doi:10.1101/gr.113985.110.

1191 61. Wick RR. Porechop v. 0.2.4. <https://github.com/rrwick/Porechop>.

1192 62. Ruan J, Li H. Fast and accurate long-read assembly with wtDBG2. *Nat Methods*.
1193 2020;17:155–8. doi:10.1038/s41592-019-0669-3.

1194 63. Li H. Minimap2: pairwise alignment for nucleotide sequences. *Bioinformatics*.
1195 2018;34:3094–100. doi:10.1093/bioinformatics/bty191.

1196 64. Abyzov A, Gerstein M. AGE: defining breakpoints of genomic structural variants at single-
1197 nucleotide resolution, through optimal alignments with gap excision. *Bioinformatics*.
1198 2011;27:595–603. doi:10.1093/bioinformatics/btq713.

1199 65. Wong K, Keane TM, Stalker J, Adams DJ. Enhanced structural variant and breakpoint

1200 detection using SVMerge by integration of multiple detection methods and local assembly.

1201 *Genome Biol.* 2010;11:R128. doi:10.1186/gb-2010-11-12-r128.

1202 66. Goodstein DM, Shu S, Howson R, Neupane R, Hayes RD, Fazo J, et al. Phytozome: a

1203 comparative platform for green plant genomics. *Nucleic Acids Res.* 2012;40:D1178–86.

1204 doi:10.1093/nar/gkr944.

1205 67. Rimmer A, Phan H, Mathieson I, Iqbal Z, Twigg SRF, Consortium W, et al. Integrating

1206 mapping-, assembly and haplotype-based approaches for calling variants in clinical sequencing

1207 applications. *Nat Genet.* 2014;46:912–8. doi:10.1038/ng.3036.

1208 68. Purcell S, Neale B, Todd-Brown K, Thomas L, Ferreira MAR, Bender D, et al. PLINK: A Tool

1209 Set for Whole-Genome Association and Population-Based Linkage Analyses. *Am J Hum Genet.*

1210 2007;81:559–75. doi:10.1086/519795.

1211 69. Raj A, Stephens M, Pritchard JK. fastSTRUCTURE: Variational Inference of Population

1212 Structure in Large SNP Data Sets. *Genetics.* 2014;197:573–89.

1213 doi:10.1534/genetics.114.164350.

1214 70. The Gene Ontology Consortium. Gene Ontology: tool for the unification of biology. *Nat*

1215 *Genet.* 2000;25:25–9. doi:10.1038/75556.

1216 71. Mistry J, Chuguransky S, Williams L, Qureshi M, Salazar GA, Sonnhammer ELL, et al.

1217 Pfam: The protein families database in 2021. *Nucleic Acids Res.* 2021;49:D412–9.

1218 doi:10.1093/nar/gkaa913.

1219 72. Falcon S, Gentleman R. Using GOstats to test gene lists for GO term association.

1220 *Bioinformatics.* 2007;23:257–8. doi:10.1093/bioinformatics/btl567.

1221 73. Carlson M. GO.db: A set of annotation maps describing the entire Gene Ontology. R

1222 package version 3.12.1. 2020. doi:10.18129/B9.bioc.GO.db.

1223 74. Du J, Grant D, Tian Z, Nelson RT, Zhu L, Shoemaker RC, et al. SoyTEdb: a comprehensive
1224 database of transposable elements in the soybean genome. *BMC Genomics*. 2010;11:113.
1225 doi:10.1186/1471-2164-11-113.

1226 75. Altschul SF, Gish W, Miller W, Myers EW, Lipman DJ. Basic local alignment search tool. *J
1227 Mol Biol*. 1990;215:403–10. doi:10.1016/S0022-2836(05)80360-2.

1228 76. Du J, Tian Z, Hans CS, Laten HM, Cannon SB, Jackson SA, et al. Evolutionary
1229 conservation, diversity and specificity of LTR-retrotransposons in flowering plants: insights from
1230 genome-wide analysis and multi-specific comparison. *Plant J*. 2010;63:584–98.
1231 doi:10.1111/j.1365-313X.2010.04263.x.

1232 77. Feschotte C, Pritham EJ. DNA Transposons and the Evolution of Eukaryotic Genomes.
1233 *Annu Rev Genet*. 2007;41:331–68. doi:10.1146/annurev.genet.40.110405.090448.

1234 78. Katoh K. MAFFT: a novel method for rapid multiple sequence alignment based on fast
1235 Fourier transform. *Nucleic Acids Res*. 2002;30:3059–66. doi:10.1093/nar/gkf436.

1236 79. Shi J, Liang C. Generic Repeat Finder: A High-Sensitivity Tool for Genome-Wide De Novo
1237 Repeat Detection. *Plant Physiol*. 2019;180:1803–15. doi:10.1104/pp.19.00386.

1238 80. R Core Team. R: A language and environment for statistical computing. R Foundation for
1239 Statistical Computing, Vienna, Austria. 2020. <https://www.r-project.org/>.

1240 81. Huber W, Carey VJ, Gentleman R, Anders S, Carlson M, Carvalho BS, et al. Orchestrating
1241 high-throughput genomic analysis with Bioconductor. *Nat Methods*. 2015;12:115–21.
1242 doi:10.1038/nmeth.3252.

1243 82. Pagès H, Aboyoun P, Gentleman R, DebRoy S. Biostrings: Efficient manipulation of
1244 biological strings. R package version 2.58.0. 2020. doi:10.18129/B9.bioc.Biostrings.

1245 83. Lawrence M, Huber W, Pagès H, Aboyoun P, Carlson M, Gentleman R, et al. Software for

1246 Computing and Annotating Genomic Ranges. PLoS Comput Biol. 2013;9:e1003118.

1247 doi:10.1371/journal.pcbi.1003118.

1248 84. Morgan M, Pagès H, Obenchain V, Hayden N. Rsamtools: Binary alignment (BAM), FASTA,
1249 variant call (BCF), and tabix file import. R package version 2.6.0. 2020.

1250 doi:10.18129/B9.bioc.Rsamtools.

1251 85. Lawrence M, Gentleman R, Carey V. rtracklayer: an R package for interfacing with genome
1252 browsers. Bioinformatics. 2009;25:1841–2. doi:10.1093/bioinformatics/btp328.

1253 86. Obenchain V, Lawrence M, Carey V, Gogarten S, Shannon P, Morgan M.

1254 VariantAnnotation: a Bioconductor package for exploration and annotation of genetic variants.

1255 Bioinformatics. 2014;30:2076–8. doi:10.1093/bioinformatics/btu168.

1256 87. Lemay M-A, Sibbesen JA, Torkamaneh D, Hamel J, Levesque RC, Belzile F.

1257 malemay/soybean_sv_paper. GitHub. 2021. https://github.com/malemay/soybean_sv_paper.

1258 88. NCBI BioProject PRJNA751911. <https://www.ncbi.nlm.nih.gov/bioproject/?term=PRJNA751911>.

1259

1260 89. Williams 82 Transposable Element Database. <https://www.soybase.org/soytedb/>.

1261 90. SoyBase Genome Annotation Report Page. <https://www.soybase.org/genomeannotation/>.

1262 91. Glycine max and G. soja BLAST database options at SoyBase.

1263 https://www.soybase.org/GlycineBlastPages/blast_descriptions.php.

1264 92. Glycine max Wm82.a4.v1. https://phytozome-next.jgi.doe.gov/info/Gmax_Wm82_a4_v1.

1265 93. Lemay M-A, Sibbesen JA, Torkamaneh D, Hamel J, Levesque RC, Belzile F. Data
1266 associated with “Combined use of Oxford Nanopore and Illumina sequencing yields insights into
1267 soybean structural variation biology.” figshare. <https://doi.org/10.6084/m9.figshare.15127730.v1>.

1268 94. Lemay M-A, Sibbesen JA, Torkamaneh D, Hamel J, Levesque RC, Belzile F.

1269 malemay/breakpoint_refinement. GitHub. https://github.com/malemay/breakpoint_refinement.

1270 95. Lemay M-A, Sibbesen JA, Torkamaneh D, Hamel J, Levesque RC, Belzile F.

1271 breakpoint_refinement. figshare. <https://doi.org/10.6084/m9.figshare.15183606.v1>.

1272 96. Lemay M-A, Sibbesen JA, Torkamaneh D, Hamel J, Levesque RC, Belzile F.

1273 soybean_sv_paper. figshare. <https://doi.org/10.6084/m9.figshare.15183570.v1>.